

Copyright © 1996, by the author(s).
All rights reserved.

Permission to make digital or hard copies of all or part of this work for personal or classroom use is granted without fee provided that copies are not made or distributed for profit or commercial advantage and that copies bear this notice and the full citation on the first page. To copy otherwise, to republish, to post on servers or to redistribute to lists, requires prior specific permission.

**CONFLICT RESOLUTION FOR AIR TRAFFIC
MANAGEMENT: A CASE STUDY IN MULTI-
AGENT HYBRID SYSTEMS**

by

Claire Tomlin, George J. Pappas, and Shankar Sastry

Memorandum No. UCB/ERL M96/38

1 July 1996

COVER PAGE

**CONFLICT RESOLUTION FOR AIR TRAFFIC
MANAGEMENT: A CASE STUDY IN MULTI-
AGENT HYBRID SYSTEMS**

by

Claire Tomlin, George J. Pappas, and Shankar Sastry

Memorandum No. UCB/ERL M96/38

1 July 1996

ELECTRONICS RESEARCH LABORATORY

College of Engineering
University of California, Berkeley
94720

Conflict Resolution for Air Traffic Management: a Case Study in Multi-Agent Hybrid Systems *

Claire Tomlin, George J. Pappas and Shankar Sastry
Department of Electrical Engineering and Computer Sciences
University of California at Berkeley
Berkeley, CA 94720
{clairet, gpappas, sastry}@eecs.berkeley.edu

Abstract

A conflict resolution architecture for multi-agent hybrid systems with emphasis on Air Traffic Management Systems (ATMS) is presented. In such systems, conflicts arise in the form of potential collisions which are resolved locally by inter-agent coordination. This results in a decentralized architecture in which safety issues are resolved locally and central agencies, such as Air Traffic Controllers, focus on global issues such as efficiency and optimal throughput. In order to allow optimization of agents' objectives, inter-agent coordination is minimized by noncooperative conflict resolution methods based on game theory. If noncooperative methods are unsuccessful, then cooperative methods in the form of coordinated maneuvers are used to resolve conflicts. The merging of inter-agent coordination, which is modeled by discrete event systems, and agent dynamics, which are modeled by differential equations, result in *hybrid systems*.

1 Introduction

We are increasingly confronted with the control of distributed multi-agent systems: such as Air Traffic Management Systems (ATMS) [1], Intelligent Vehicle Highway Systems (IVHS) [2], control systems of an interconnected power grid, and communication networks. Let us for the sake of specificity focus on the first two systems: the common feature of these systems is that agents compete for usage of a common resource, such as space time on the jetways, airport runways, highways, etc. There is a need to balance individual safety of the agents with system level optimality of the utilization of the scarce resource. Indeed, as we have all observed in driving, the optimal greedy policies of individual agents result in conflict and loss of optimal utilization of the common resource as a whole.

One of the most important conceptual issues to be addressed in the architecture of these control systems is their degree of decentralization. The foregoing examples are revealing: current air traffic control practice is completely centralized (with the regional centers, airport control towers, gate controllers) providing all of the instructions, while current roadway driving practice is completely

*Research supported by the Army Research Office under grant DAAH 04-95-1-0588 and by NASA under grant NAG2-243.

decentralized with individual drivers (usually adopting “greedy strategies”) setting their driving control laws. There are clear drawbacks to each: the completely decentralized solution is *inefficient and leads to conflict*, the completely centralized control laws are *not tolerant of faults in the central controller, computationally and conceptually complicated and slow to respond to emergencies*. The focus of our research has been to strike a compromise in the form of partially decentralized control laws for guaranteeing *reliable, safe control of the individual agents* while providing *some measure of unblocked, fair, and optimum utilization of the scarce resource*. In our design paradigm, agents have control laws to maintain their safe operation, and try to optimize their own performance measures. They also coordinate with neighboring agents and a centralized controller to resolve conflicts as they arise and maintain efficient operation.

For reasons of economic and reliable information transfer among the agents and the centralized controller, coordination among the agents is usually in the form of communication protocols which are modeled by discrete event systems. Since the dynamics of individual agents is modeled by differential equations, we are left with a combination of interacting discrete event dynamical systems and differential equations resulting in *hybrid control systems*. An important issue in the area of hybrid systems is the analysis and design of protocols and interfaces between agents as well as continuous control laws for each agent. Continuous control laws are usually proven correct by traditional tools of control theory, whereas verification of coordination protocols is performed by computer verification algorithms (such as in [3], [4]). There are several approaches to hybrid system design and verification (see for example [5, 6]). One approach is to extend verification techniques which exist for finite state machines [3] to include timed and dynamical systems. These approaches abstract the differential equations by clocks [7] or differential inclusions [8] and verify the resulting abstracted system. More unified approaches in which the hybrid system design is not decoupled into the design of the individual continuous and discrete components are [9, 10, 11, 12, 13].

A natural framework for formulating problems in which many agents have different objectives is game theory [14, 15]. Consider at the outset the simplest kind of game: a noncooperative zero-sum dynamic game with each agent is modeled as a player [16]. In this framework, each agent treats every other agent (for the sake of pairwise interactions) as a disturbance. Assuming a saddle solution to the game exists, the agent chooses an optimal policy assuming the worst possible disturbance. The resulting solution involves switching between different modes of operation and can be represented as a hybrid automaton. For multiple agent coordination, the kinds of games that need to be considered are *cooperative and competitive* with possibly *incomplete information*. For such games, there is a large literature available (see for example [17]), but our approach would be to try to find ways of abstracting the solutions of the games in the form of *protocols* among the agents. The extent to which the protocol is centralized or decentralized is an interesting question to answer. Game theoretic methods have been used in a similar way to prove that a set of maneuvers in Intelligent Vehicle Highway Systems is safe [18], [19].

The current paper studies conflict resolution for aircraft in the context of a new architecture for Air Traffic Management that has been proposed in [1] to allow for some shift away from the traditional completely centralized Air Traffic Control paradigm. It has been motivated by some estimates from commercial airline sources of savings of close to \$15 billion in the United States alone which would accrue from allowing for so-called “free flight” off the current pre-assigned jetways. Even in the crowded air space over Western Europe, where free flight is not as important a consideration, it has been estimated that allowing for more air traffic control functions to be performed in decentralized fashion on board the aircraft will result in much faster system response and consequent savings on expensive holding patterns. Related studies in new air traffic management systems include [20] and

[21].

The organization of this paper is as follows. In Section 2, a conflict resolution architecture for multi-agent path planning systems is described. Long range collision avoidance among aircraft is noncooperative and is modeled as a zero-sum game. The performance requirement in this case is encoded by the distance between two agents which should never fall below a minimum threshold. The long range collision avoidance maneuvers are chosen to be maximally decentralized, i.e. "on board". As the range gets shorter, or when the long range conflict resolution maneuvers fail, coordination (cooperation) among the agents is used and multiple agent coordination strategies are discussed. Finally, the fully centralized Air Traffic Control strategy is also utilized in our framework. In Section 3, the agents are kinematically modeled as elements of the Lie groups $SE(2)$ and $SE(3)$. Section 4 describes a noncooperative zero sum game approach to long range collision avoidance. The solution of the game is abstracted into a finite state automaton, and the composite hybrid system is safe by design, obviating the need for further verification. Section 5 describes the predefined, coordinated maneuvers which guarantee collision avoidance at short range. For two aircraft, the protocols were derived using two "pilot inspired" maneuvers for overtaking and head-on conflict avoidance. They involve coordination between the two aircraft, but no others that are outside the "alert zone". The use of a verification tool developed at Berkeley called HyTech in verifying the design is indicated. We also extend the HeadOn conflict resolution protocol to multiple aircraft agents. These extensions have not yet been verified on HyTech, but are expected to be safe. In the design of these protocols, we have realized the important connections that they make with Nash solutions of non-competitive games, but have not yet worked out all the details. Our results, with their attractive features for current pilot and Air Traffic Control practice, represent an important first step in finding abstractions to cooperative games which represent trajectories that pilots find easy to fly. Section 6 discusses issues for further research.

2 Conflict Resolution Architecture

In multi-agent path planning problems, the agents wish to traverse different trajectories which have been designed in an optimal fashion according to the goals of each agent [22, 23, 24]. Very frequently, however, the trajectories of two or more agents may be collision bound, in which case the planned trajectories must be altered in order to avoid collision.

In particular, in current air traffic systems, conflict resolution is performed centrally by Air Traffic Control (ATC). Centralized control schemes are theoretically more efficient than decentralized schemes if all information is available to the central decision maker. However, centralization comes at the cost of extreme complexity, amplified by current computation and communication limitations. Air traffic controllers have the highly stressful task of manually guiding and sequencing many aircraft through their *sectors* of airspace. In an effort to reduce the complexity, the system is simplified. ATC routes aircraft along well-traveled jetways, and avoids the problems of multi-aircraft conflict by placing many aircraft in holding patterns. The simplification of the complex, global system model results in suboptimal or inefficient solutions which may defeat the purpose of having centralized schemes. Also, centralized schemes are not reliable since any malfunction of the centralized decision maker is hazardous to all associated agents¹.

¹Indeed, in August 1995, the central computer controlling the air traffic in the FAA Fremont control center experienced a 65 minute power failure, leaving close to 70 aircraft with no communication to ATC.

On the other hand, decentralized control schemes distribute the problem complexity to all associated agents. The computational complexity at the level of each individual agent is clearly less than is required by the central decision maker in a centralized scheme. However, this also requires proper distribution of computational power as well as an increase in inter-agent communication. Fortunately enough, this is permitted by current technological advances (Global Positioning Systems (GPS), Flight Management Systems (FMS)) which enable the implementation of decentralized architectures. In addition, decentralized schemes are more fault tolerant than centralized schemes, since malfunctions are of a local nature and can be potentially hazardous only to the malfunctioning aircraft as well as to some neighboring aircraft.

The design of a conflict resolution architecture has to choose a proper balance between centralized and decentralized authority. Central agencies are concerned with global issues while decentralized agencies are concerned with local problems. For multi-agent path planning problems, a conflict takes the form of a potential collision which is essentially a local property and it seems natural to address this problem at a decentralized level. *We therefore propose a conflict resolution architecture in which conflicts are resolved locally by inter-agent coordination.*

In this type of architecture, central agencies can focus on more global issues such as optimality; by avoiding local questions, the complexity of the problem is reduced. This complexity reduction may result in converting suboptimal solutions of the complex optimization problem to optimal solutions of a simplified problem. In addition, central control can offer advice in safety critical situations which may not be resolved locally. The central agency can also serve as a backup in case there are local inter-agent malfunctions. This, in addition to the natural fault tolerance of decentralized structures, will result in increased overall system safety and reliability.

In a multi-agent society, different agents are interested in different objectives which may be conflicting. Although conflicts will be resolved locally among agents, it is rather clear that the success of such an architecture will depend on the relative time that each agent is allowed to optimize its own goals. *It is therefore desirable to minimize inter-agent interaction.* For path planning problems, this will allow aircraft to stay on their nominal optimized trajectories for as long as possible.

Inter-agent coordination is minimized by classifying conflicts according to whether they are *long range* or *short range*, and by attempting to resolve long range conflicts without any coordination among agents. In the path planning problems addressed in this paper, long range conflict resolution acts a *filter* which, by adjusting the velocities of the agents within given bounds, reduces the number of conflicts which have to be considered at short range. Short range conflicts are more safety critical than long range, and must be solved by coordination among the agents.

The notions just discussed, of centralized vs. decentralized control schemes, local vs. global system properties, and short range vs. long range conflict, are captured in the proposed hierarchical architecture for conflict resolution of Figure 1. The algorithms contained within this architecture, the subject of the rest of this paper, are resident in and are executed by each agent in the system. In Air Traffic Management Systems, the algorithms reside in the *Flight Vehicle Management System* (FVMS) located on board each aircraft.

As the agents referred to in this paper are actually aircraft in an air traffic system, *long range* and *short range* are conveniently depicted according to the sensor and communication ranges shown in Figure 2:

- *Detection Zone (approx. 100 miles):* The detection zone is defined by the radius of the aircraft's sensing capability. Conflicts within this region are classified as *long range* and are

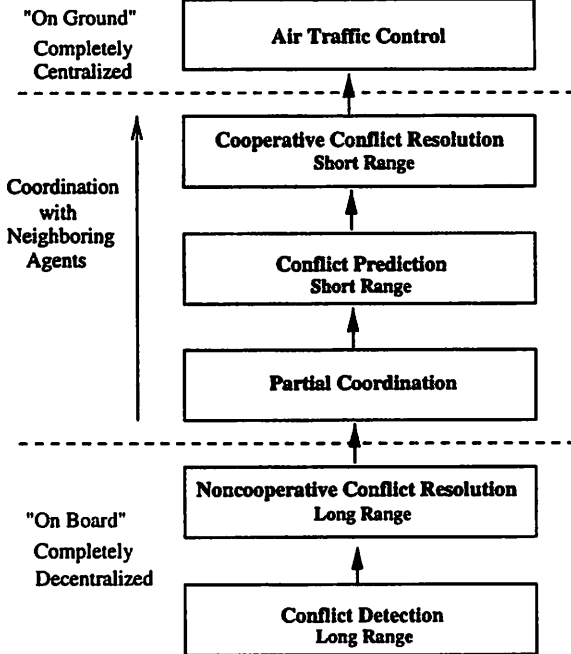


Figure 1: Conflict Resolution Architecture

resolved noncooperatively by small velocity variations which over the long range horizon will result in sufficiently large spacings between aircraft.

- *Alert Zone (approx. 30 miles)*: Conflicts within this region are classified as *short range*. Within this zone, conflicts are resolved cooperatively using more drastic maneuvers such as altitude and/or direction changes.
- *Protected Zone (approx. 2.5 miles)*: A collision between two aircraft occurs when their respective protected zones have nonempty intersection. Therefore, protected zones essentially provide a minimum safety distance between aircraft.

At the lowest level of the architecture, long range *Conflict Detection* is performed. Conflict detection is based on sensory information available to the aircraft, which detects the instantaneous position and heading of each aircraft within the *Detection Zone* around the given aircraft. The state of the art detection technology is FAA's tool called TCAS, which transmits its own IP signal and receives other aircrafts' ID signals from within a given vicinity. Once this set of agents involved in potential conflicts has been identified, it is assumed that no new agents will enter the set until all conflicts have been resolved. In the case in which new agents are likely to enter the set, an extended problem which includes these agents in the formulation will be considered.

The first attempt to resolve the conflict is to perform *Noncooperative Conflict Resolution* with no coordination between the agents. The agents are treated as players in a n-player, zero-sum noncooperative dynamic game. Each player is aware only of the possible actions of the other agents. These actions are modeled as disturbances, assumed to lie within a known set but with their particular values unknown and uncontrolled. Each agent solves the game considering the worst possible disturbance. The performance index over which the agents are competing is the relative distance between the agents, required to be above a certain threshold which is determined



Figure 2: Aircraft Zones

by the size of the protected zone. Assuming that a saddle solution to the game exists, the saddle solution is *safe* if the performance index evaluated at the saddle solution is above the required threshold. In this case the agent follows the policy dictated by the saddle solution and does not have to coordinate with the other agents. If the saddle solution to the game is unsafe, it may be because the disturbance sets are too large. *Partial Coordination* between the agents is then necessary in order to reduce the disturbance sets. We distinguish between collision avoidance among *heterogeneous agents* and *homogeneous agents*.

Heterogeneous agents are linearly ranked according to some priority system. Priorities are assigned after considering economic factors, emergency situations, and maneuverability of various agents. In this case, the agents may choose their own policies as long as they do not interfere with the policies of the higher ranked agents. The agents are therefore aware of the actions of higher ranked opponents. From a game theoretic viewpoint this simply results in reducing the disturbance sets to known functions of time and the game is thus reduced to an optimal control problem. If the agents are homogeneous, then every agent transmits to all other agents the disturbance sets for which a safe solution exists for its game. If the intersection of these reduced disturbance sets is nonempty then collision can be avoided by simply reducing the possible actions of each agent.

If reducing the disturbance set still results in an unsafe solution, *Cooperative Conflict Resolution* is necessary. In this scenario, optimality considerations become less significant and safety is ensured by full coordination among all of the agents. Short range *Conflict Prediction* is first performed to determine the point of collision. The agents then follow predefined maneuvers which are proven to be safe. These maneuvers are a combination of a verified communication protocol as well as control laws. The class of maneuvers constructed to resolve conflicts must be rich enough to cover most possible conflict scenarios. Furthermore, different maneuvers may be constructed for resolving conflicts among heterogeneous agents rather than among homogeneous agents.

At the top of the hierarchy is the centralized ATC, which will intervene and attempt to resolve a conflict if it cannot be resolved by Cooperative Conflict Resolution among agents.

3 Modeling

Because conflicts between agents depend on the relative position and velocity of the agents, it is useful in the following analysis to derive *relative* kinematic models, describing the motion of each aircraft in the system with respect to the other aircraft. For example, to study pairwise conflict between the trajectories of two aircraft, aircraft 0 and aircraft 1, a relative model with its origin centered on aircraft 0 is used. The parameters of the model, such as the velocity of aircraft 1, may not be known to aircraft 0, yet aircraft 0 has estimates on the bounds of these parameters, which it can use in noncooperative collision avoidance.

The configuration of an individual agent is described by an element of a Lie group G . The Lie group G will typically be either the group of rigid motions in \mathbb{R}^2 or \mathbb{R}^3 , called $SE(2)$ or $SE(3)$ respectively. In planar situations, in which aircraft are flying at the same altitude, $SE(2)$ will be used.

Following the example described above, let $g_0 \in G$ denote the configuration of aircraft 0, and let $g_1 \in G$ denote the configuration of aircraft 1. The trajectories of both aircraft are kinematically modeled as left invariant vector fields on G . Therefore

$$\dot{g}_0 = g_0 X_0 \quad (1)$$

$$\dot{g}_1 = g_1 X_1 \quad (2)$$

where $X_0, X_1 \in \mathcal{G}$, the Lie algebra associated with the Lie group G .

A coordinate change is performed to place the identity element of the Lie group G on aircraft 0. Thus, let $g_r \in G$ denote the relative configuration of aircraft 1 with respect to aircraft 0. Then

$$g_1 = g_0 g_r \Rightarrow g_r = g_0^{-1} g_1 \quad (3)$$

Differentiation yields the dynamics of the relative configuration,

$$\dot{g}_r = g_r X_1 - X_0 g_r \quad (4)$$

Note that the vector field which describes the evolution of g_r is neither left nor right invariant. However,

$$\begin{aligned} \dot{g}_r &= g_r X_1 - X_0 g_r \\ &= g_r [X_1 - Ad_{g_r^{-1}} X_0] \end{aligned} \quad (5)$$

where $Ad_{g_r^{-1}} X_0 = g_r^{-1} X_0 g_r \in \mathcal{G}$.

Consider the Lie group $SE(2)$ and its associated Lie algebra $se(2)$. A coordinate chart for $SE(2)$ is given by x, y, θ representing the planar position and orientation of a rigid body. In this coordinate chart, the relative configuration g_r is given in homogeneous coordinates by

$$g_r = \begin{bmatrix} \cos \theta_r & -\sin \theta_r & x_r \\ \sin \theta_r & \cos \theta_r & y_r \\ 0 & 0 & 1 \end{bmatrix} \quad (6)$$

where x_r, y_r represent the relative position of aircraft 1 with respect to aircraft 0 and θ_r is the relative orientation. The Lie algebra elements $X_0, X_1 \in se(2)$ are represented as matrices in $\mathbb{R}^{3 \times 3}$

of the form

$$X_0 = \begin{bmatrix} 0 & -\omega_0 & v_0 \\ \omega_0 & 0 & 0 \\ 0 & 0 & 0 \end{bmatrix} \quad X_1 = \begin{bmatrix} 0 & -\omega_1 & v_1 \\ \omega_1 & 0 & 0 \\ 0 & 0 & 0 \end{bmatrix} \quad (7)$$

where v_i, ω_i represent the translational and rotational velocities. Inserting equations (6) and (7) in equation (4) results in the following model

$$\begin{aligned} \dot{x}_r &= -v_0 + v_1 \cos \theta_r + \omega_0 y_r \\ \dot{y}_r &= v_1 \sin \theta_r - \omega_0 x_r \\ \dot{\theta}_r &= \omega_1 - \omega_0 \end{aligned} \quad (8)$$

Now consider the Euclidean group $SE(3)$ along with its associated Lie algebra $se(3)$. A coordinate chart for $SE(3)$ is given by $x, y, z, \phi, \theta, \psi$ representing the planar position and orientation. The orientation is parameterized using the yaw-pitch-roll chart where ψ is the yaw, θ is the pitch and ϕ is the roll. In this coordinate chart, the relative configuration g_r is given in homogeneous coordinates by

$$g_r = \begin{bmatrix} C\psi_r C\theta_r & C\psi_r S\theta_r S\phi_r - S\psi_r C\phi_r & C\psi_r S\theta_r C\phi_r + S\phi_r S\psi_r & x_r \\ S\psi_r C\theta_r & S\psi_r S\theta_r S\phi_r + C\psi_r C\phi_r & S\psi_r S\theta_r C\phi_r - S\phi_r C\psi_r & y_r \\ -S\theta_r & C\theta_r S\phi_r & C\theta_r C\phi_r & z_r \\ 0 & 0 & 0 & 1 \end{bmatrix} \quad (9)$$

where x_r, y_r, z_r represent the relative position of aircraft 1 in the coordinate system which is attached to aircraft 0 and ϕ_r, θ_r, ψ_r parameterize the relative orientation. In equation (9), the notation $S\alpha$ stands for the sine of the angle α and $C\alpha$ for the cosine. The Lie algebra elements $X_0, X_1 \in se(3)$ are of the following form

$$X_0 = \begin{bmatrix} 0 & -\omega_3^0 & \omega_2^0 & v_0 \\ \omega_3^0 & 0 & -\omega_1^0 & 0 \\ -\omega_2^0 & \omega_1^0 & 0 & 0 \\ 0 & 0 & 0 & 0 \end{bmatrix} \quad X_1 = \begin{bmatrix} 0 & -\omega_3^1 & \omega_2^1 & v_1 \\ \omega_3^1 & 0 & -\omega_1^1 & 0 \\ -\omega_2^1 & \omega_1^1 & 0 & 0 \\ 0 & 0 & 0 & 0 \end{bmatrix} \quad (10)$$

where $v_i, \omega_1^i, \omega_2^i, \omega_3^i$ represent the translational and rotational velocities. Inserting equations (9) and (10) in equation (4) results in the following model

$$\begin{aligned} \dot{x}_r &= -v_0 - \omega_3^0 y_r - \omega_2^0 z_r + v_1 \cos \psi_r \cos \theta_r \\ \dot{y}_r &= -\omega_3^0 x_r + \omega_1^0 z_r + v_1 \sin \psi_r \cos \theta_r \\ \dot{z}_r &= \omega_2^0 x_r - \omega_1^0 y_r - v_1 \sin \theta_r \\ \dot{\theta}_r &= -\omega_2^0 C\psi_r + \omega_2^1 C\phi_r + \omega_1^0 S\psi_r - \omega_3^1 S\phi_r \\ \dot{\psi}_r &= -\omega_3^0 + \frac{1}{C\theta_r} [-\omega_2^0 S\psi_r S\theta_r + \omega_2^1 S\phi_r + \omega_3^1 C\phi_r - \omega_1^0 C\psi_r S\theta_r] \\ \dot{\phi}_r &= \omega_1^1 + \frac{1}{C\theta_r} [\omega_3^1 C\phi_r S\theta_r - \omega_2^0 S\psi_r - \omega_1^0 C\psi_r + \omega_2^1 S\phi_r S\theta_r] \end{aligned} \quad (11)$$

Notice that equations (11) are ill posed when $\theta_r = \pm \frac{\pi}{2}$ as expected from the singularity of the yaw-pitch-roll parameterization of $SE(3)$.

4 Noncooperative Conflict Resolution

4.1 Game Theoretic Approach

In this section, a method for noncooperative conflict resolution among agents based on [16] is presented. Agents are aware of the relative position and heading of neighboring agents but not of their velocities. The following methodology is used as a long range collision avoidance scheme in an effort to filter all conflicts that can be resolved without inter-agent cooperation.

A two agent scenario is considered. Scenarios involving more agents, although considerably more complex, are conceptually similar. Let

$$\dot{x} = f(x, u, d, t) \quad x(t_0) = x_0 \quad (12)$$

model the dynamics of the relative configuration $x \in \mathbb{R}^n$ between the two agents, where $u \in \mathcal{U}$ is the control input of one agent, called the *evader*, and $d \in \mathcal{D}$ is the control of the other agent, called the *pursuer*. The actions of the evader are controlled whereas the actions of the pursuer are *unknown and uncontrollable* but are known to lie within the disturbance set \mathcal{D} . Thus, the actions of the evader are modeled as control inputs whereas the actions of the pursuer as disturbances.

The requirement for collision avoidance is encoded in a cost function $J_s(x_0, u, d)$ and is simply the distance between the two agents. A trajectory of system (12) is called *safe* if

$$J_s(x_0, u, d) \geq C \quad (13)$$

for some constant C determined by the size of the protected zones. In a zero-sum, noncooperative game, the pursuer tries to minimize the distance between the agents whereas the evader tries to maximize it.

A saddle solution to the game exists when there exists input u^* and disturbance d^* such that

$$\begin{aligned} J_s(x_0, u^*, d^*) &= \max_{d \in \mathcal{D}} \min_{u \in \mathcal{U}} J_s(x_0, u, d) \\ &= \min_{u \in \mathcal{U}} \max_{d \in \mathcal{D}} J_s(x_0, u, d) \end{aligned}$$

If a saddle solution exists, the optimal policy for the evader is u^* whereas the worst possible disturbance by the pursuer is d^* . If the trajectory of (12) corresponding to the saddle solution (u^*, d^*) is safe, then collision is avoided by the evader for the worst possible pursuer disturbance. In this case, collision is avoided regardless of what the pursuer will do as long as the evader chooses its optimal policy. *This allows the evader to choose a control policy which guarantees safety without having to communicate or cooperate with the pursuer.* This is the fundamental idea in noncooperative conflict resolution and results in minimal inter-agent interaction.

The safety of a particular control policy also depends on the initial relative configuration x_0 . The set of safe initial relative configurations is defined as

$$V_s = \{x_0 \in \mathbb{R}^n | J_s(x_0, u^*, d^*) \geq C\} \quad (14)$$

If the initial relative configuration does not belong in V_s then collision avoidance is not guaranteed. In that case, noncooperative methods alone will not suffice. If, however, $x_0 \in V_s$ then safety is guaranteed by choosing the control policy u^* . In general, given an initial relative configuration $x_0 \in V_s$, the following set

$$\mathcal{U}_s(x_0) = \{u \in \mathcal{U} | J_s(x_0, u, d^*) \geq C\} \quad (15)$$

is defined as the set of control policies which guarantee safety from relative configuration x_0 . Since all $u \in \mathcal{U}_s(x_0)$ guarantee safety from x_0 , it is advantageous to find the control policy $u \in \mathcal{U}_s(x_0)$ which minimizes deviation from the nominal trajectory. Deviation from the nominal trajectory is encoded in a cost function J_e which is usually a quadratic function of the tracking error. Therefore, minimization of the tracking error which guarantees safety from relative configuration x_0 , is performed by solving the following optimal control problem

$$\min_{u \in \mathcal{U}_s(x_0)} J_e \quad (16)$$

subject to the differential equations (1,2) which describe the dynamics of individual agents in absolute coordinates and can therefore be used to describe the tracking error dynamics.

Additional system requirements such as passenger comfort can also be incorporated by extending the above nested chain of games and optimal control problems [16]. The above methodology is now illustrated in the instance of planar conflict resolution.

4.2 Planar Conflict Resolution

Suppose we consider the special but interesting case of model (8) in which $\omega_i = 0$, $i = 0, 1$. The agents are restricted to straight line motion, which, for example, corresponds to two aircraft flying along straight lines at the same altitude. Conflicts can then be resolved by altering velocity variations. The model then reduces to

$$\begin{aligned} \dot{x}_r &= -v_0 + v_1 \cos \theta_r \\ \dot{y}_r &= v_1 \sin \theta_r \\ \dot{\theta}_r &= 0 \end{aligned} \quad (17)$$

where v_0 is the speed of the evader, v_1 is the speed of the pursuer, and the constant θ_r represents the relative orientation between the evader and the pursuer.

In this problem, v_0 is the control and v_1 is considered the disturbance. Collision is essentially avoided by altering the velocity profile of the trajectories. The input and disturbance lie in closed subsets of the positive real line,

$$v_0 \in \mathcal{U} = [\underline{v}_0, \bar{v}_0] \subset \mathbb{R} \quad (18)$$

$$v_1 \in \mathcal{D} = [\underline{v}_1, \bar{v}_1] \subset \mathbb{R} \quad (19)$$

In the case in which the agents are aircraft, we have $\underline{v}_0 > 0$ and $\underline{v}_1 > 0$. Equations (17) can be integrated to give

$$\begin{aligned} x_r(t) &= x_r(0) - \int_0^t v_0(\tau) d\tau + \cos \theta_r \int_0^t v_1(\tau) d\tau \\ y_r(t) &= y_r(0) + \sin \theta_r \int_0^t v_1(\tau) d\tau \\ \theta_r(t) &= \theta_r(0) \end{aligned} \quad (20)$$

and when v_0 and v_1 are constant,

$$\begin{aligned} x_r(t) &= x_r(0) + (-v_0 + v_1 \cos \theta_r)t \\ y_r(t) &= y_r(0) + (v_1 \sin \theta_r)t \\ \theta_r(t) &= \theta_r(0) \end{aligned} \quad (21)$$

From now on, let $q = [x, y, \theta]^T$ denote the state with q_0 denoting the initial state. The requirement for collision avoidance is encoded in the cost function J_s ,

$$J_s(q_0, v_0, v_1) = \inf_{t \geq 0} (|x_r(t)| + |y_r(t)|) \quad (22)$$

which is a measure of the distance between the pursuer and the evader. To avoid collisions, we require

$$J_s(q_0, v_0, v_1) \geq C, \quad (23)$$

where C describes a safety distance margin around the agents and is determined by the radius of the protected zones. Note that since the L_1 norm is used in (22), the threshold constant C must be large enough in order to include the protected zone.

The optimal policy for both the evader and the pursuer will correspond to a saddle point of the optimizing cost. It is clear from the dynamics that the saddle solution will depend on the position and orientation of the pursuer with respect to the evader.

Proposition 1 [Saddle Solution] *The global saddle solution (v_0^*, v_1^*) to the game described by system (17) for the cost $J_s(q_0, v_0, v_1)$ given by equation (22) is*

$$v_0^* = \begin{cases} \underline{v}_0 & \text{if } \operatorname{sgn}(x_r) > 0 \\ \bar{v}_0 & \text{if } \operatorname{sgn}(x_r) < 0 \end{cases} \quad (24)$$

$$v_1^* = \begin{cases} \underline{v}_1 & \text{if } \operatorname{sgn}(x_r) \cos \theta_r + \operatorname{sgn}(y_r) \sin \theta_r > 0 \\ \bar{v}_1 & \text{if } \operatorname{sgn}(x_r) \cos \theta_r + \operatorname{sgn}(y_r) \sin \theta_r < 0 \end{cases} \quad (25)$$

Proof: In Appendix. \square

As can be seen from equation (24), the optimal control depends on the position of the pursuer relative to the evader. If the pursuer is ahead of the evader then the evader should move as slowly as possible whereas if the pursuer is behind the evader then the evader should move as quickly as possible. The worst possible disturbance is described by equation (25). Simple trigonometric calculations show that

$$(\operatorname{sgn}(x_r) \cos \theta_r + \operatorname{sgn}(y_r) \sin \theta_r) = \operatorname{sgn}(y_r) \sqrt{2} \sin[\theta_r + \operatorname{sgn}(x_r y_r) \frac{\pi}{4}] \quad (26)$$

Therefore, if x_r and y_r have the same sign, then the sign of $\sin(\theta_r + \frac{\pi}{4})$ is used in determining the pursuer's policy whereas if x_r and y_r have opposite signs then it is the sign of $\sin(\theta_r - \frac{\pi}{4})$ that is used. Equations (25) and (26) may be interpreted intuitively as follows: if the pursuer is heading towards the evader, then the pursuer moves as quickly as possible; if heading away from the evader, the pursuer should move as slowly as possible. This is shown in Figure 3.

Notice that the bang-bang nature of the saddle solution allows us to abstract the system behavior by the hybrid automaton shown in Figure 4. The automaton switches between four different discrete states and within each state, there exists a differential equation, namely equation (17) with v_0 and v_1 as shown in Figure 4. The invariance conditions for each state are obtained from equations (24,25) and are summarized in the following table. If the invariance conditions for the current discrete state are not satisfied, then the hybrid automaton is forced to switch to the state where the invariance conditions are satisfied.

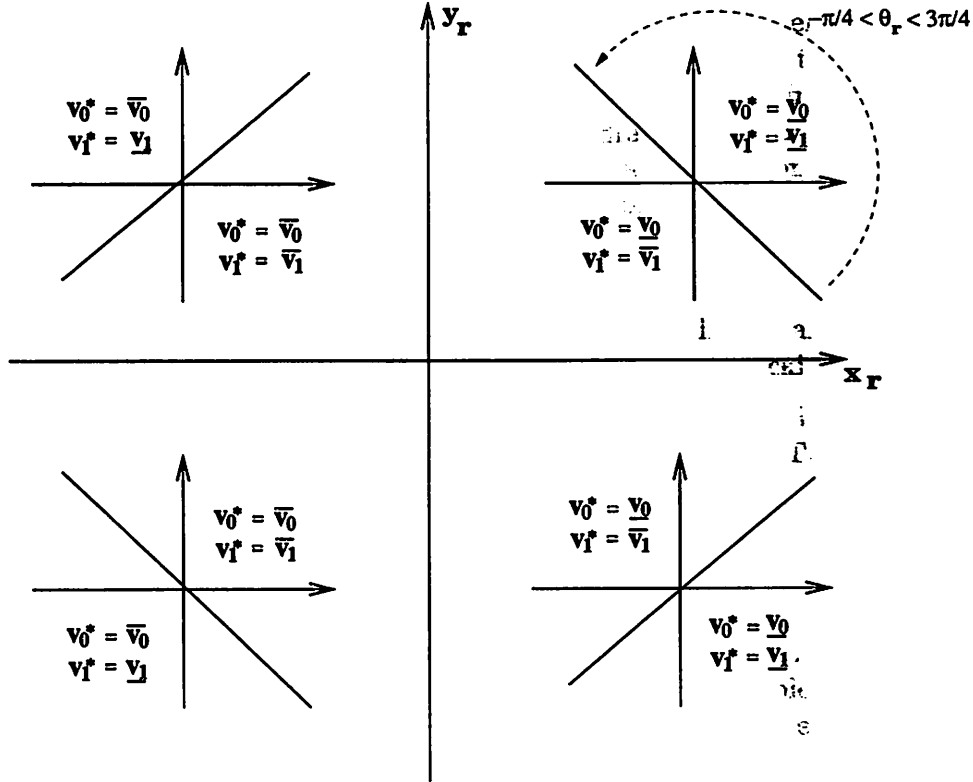


Figure 3: Interpretation of Optimal Control and Worst Disturbance (v_0^*, v_1^*)

Discrete State	Invariance Conditions
PURSUER AHEAD AND HEADING TOWARDS	$sgn(x_r) \cos \theta_r + sgn(y_r) \sin \theta_r < 0$ $sgn(x_r) > 0$
PURSUER AHEAD AND HEADING AWAY	$sgn(x_r) \cos \theta_r + sgn(y_r) \sin \theta_r > 0$ $sgn(x_r) > 0$
PURSUER BEHIND AND HEADING TOWARDS	$sgn(x_r) \cos \theta_r + sgn(y_r) \sin \theta_r < 0$ $sgn(x_r) < 0$
PURSUER BEHIND AND HEADING AWAY	$sgn(x_r) \cos \theta_r + sgn(y_r) \sin \theta_r > 0$ $sgn(x_r) < 0$

It is also possible to have diagonal transitions in the automaton of Figure 4. These transitions, however, are triggered only when both the pursuer and the evader change policy simultaneously. From equations (24) and (25) it is clear that this happens only when the pursuer crosses through the origin, in which case a collision has occurred.

It is clear from the feedback laws (24,25) that the resulting closed loop system is described by a discontinuous differential equation. The surfaces of discontinuity, as can be seen from equations (24,25), are simply the x_r - and y_r -axes. The following proposition establishes conditions under which chattering solutions in the sense of Filippov are possible.

Proposition 2 [Chattering Saddle Solutions] Consider the relative configuration model (17)

$$\dot{x}_r = -v_0 + v_1 \cos \theta_r$$

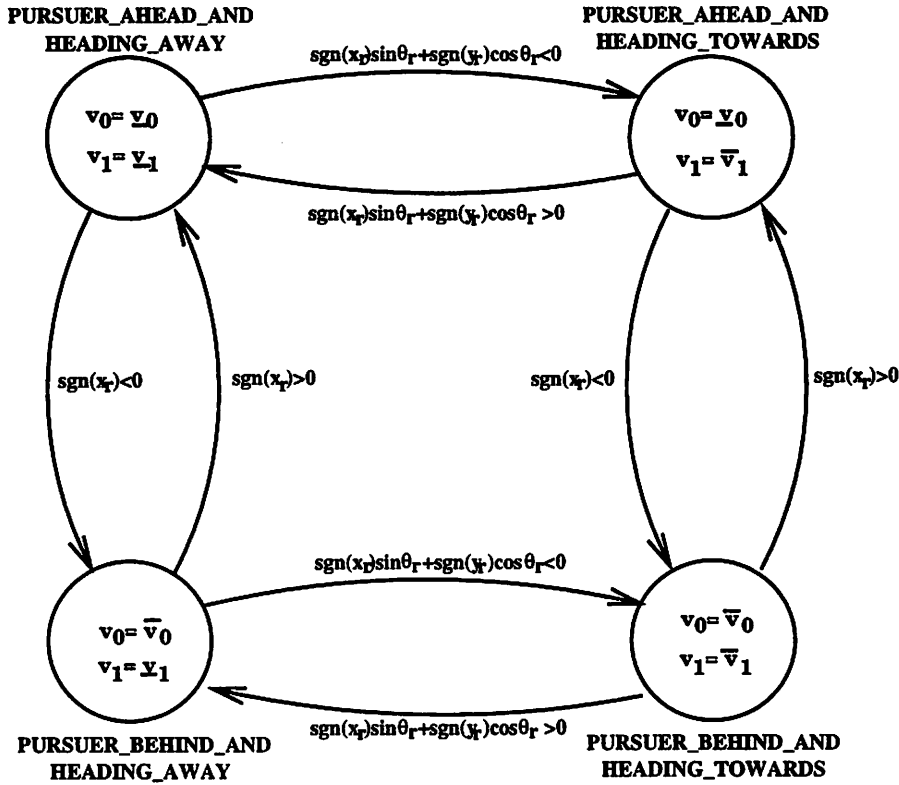


Figure 4: Abstraction of Saddle Solution as a Hybrid Automaton

$$\dot{y}_r = v_1 \sin \theta_r$$

with control laws (24,25),

$$v_0^* = \begin{cases} \underline{v}_0 & \text{if } \text{sgn}(x_r) > 0 \\ \bar{v}_0 & \text{if } \text{sgn}(x_r) < 0 \end{cases}$$

$$v_1^* = \begin{cases} \underline{v}_1 & \text{if } \text{sgn}(x_r) \cos \theta_r + \text{sgn}(y_r) \sin \theta_r > 0 \\ \bar{v}_1 & \text{if } \text{sgn}(x_r) \cos \theta_r + \text{sgn}(y_r) \sin \theta_r < 0 \end{cases}$$

Then the x_r -axis ($\{(x_r, y_r) \in \mathbb{R}^2 | y_r = 0\}$) is a chattering surface only if ²

$$\sin \theta_r \neq 0 \text{ and } \underline{v}_1 < 0 < \bar{v}_1 \quad (27)$$

and the y_r -axis ($\{(x_r, y_r) \in \mathbb{R}^2 | x_r = 0\}$) is a chattering surface only if either

$$\cos \theta_r < 0 \text{ and } \underline{v}_1 \cos \theta_r > \bar{v}_0 \text{ and } \bar{v}_1 \cos \theta_r < \underline{v}_0 \quad (28)$$

or

$$\cos \theta_r > 0 \text{ and } \bar{v}_1 \cos \theta_r > \bar{v}_0 \text{ and } \underline{v}_1 \cos \theta_r < \underline{v}_0 \quad (29)$$

²Note that condition (27) does not apply to aircraft.

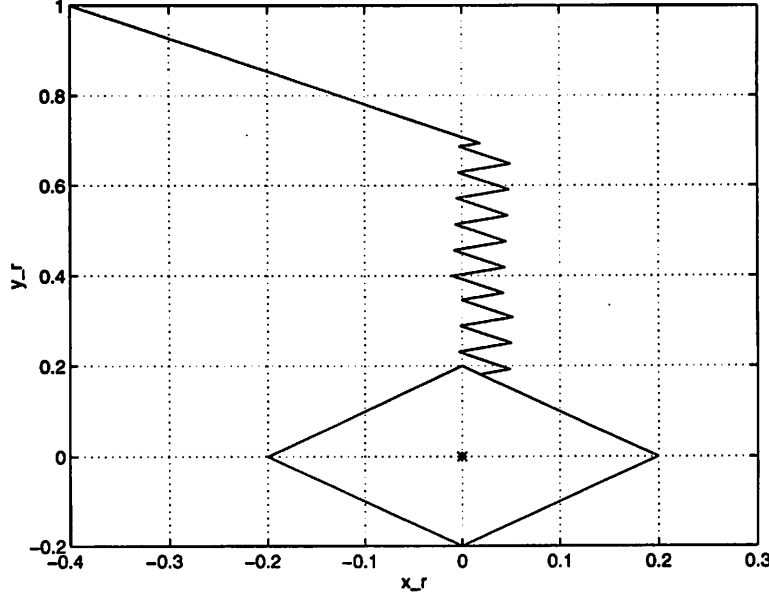


Figure 5: Chattering Solution for $[\underline{v}_0, \bar{v}_0] = [2, 4]$, $[\underline{v}_1, \bar{v}_1] = [1, 10]$, $\theta_r = -\pi/8$ and $C = 0.2$.

Proof: In Appendix. \square

From condition (27), it is clear that the x_r -axis is a chattering surface only if the pursuer can move both forwards and backwards and does not move parallel to the evader. If the pursuer cannot move backwards, as in the case of aircraft, then the x_r -axis cannot be a chattering surface. However, conditions (28,29) are feasible even when the agents are aircraft with $\underline{v}_0 > 0$, $\underline{v}_1 > 0$ as long as the disturbance set is sufficiently larger than the control set. In other words, chattering is possible when the pursuer has sufficiently more control authority than the evader and, thus, the pursuer can move both faster and slower than the evader. In that case, as shown in Figure 5, the saddle solutions initially move towards the y_r -axis, and once the solution reaches the y_r -axis then chattering occurs and the averaged solution moves along the y_r -axis, either towards or away the evader depending on the relative configuration. If the relative orientation is such that the averaged trajectory of the pursuer moves towards the evader along the y_r -axis then collision is guaranteed. Therefore, for chattering solutions, the question of collision avoidance can be answered by geometric reasoning since all that is required to know is where the pursuer hits the y_r -axis and what the relative orientation is.

Having calculated the optimal policies for both the pursuer and the evader, one can find initial conditions for which the game is won by the evader and therefore collision is avoided regardless of what the pursuer does. Define the safe set of initial conditions as

$$V_s = \{(x_r(0), y_r(0)) \in \mathbb{R}^2 \mid J_s(x_r(0), y_r(0), v_0^*, v_1^*) \geq C\} \quad (30)$$

The analytic calculation of V_s is now demonstrated. Consider the representative case, depicted in Figure 6 where the initial position of the pursuer is such that $x_r(0) > 0$, $y_r(0) > 0$, and the relative angle is $\theta_r \in (\pi, \frac{3\pi}{2})$ so that $\cos \theta_r < 0$ and $\sin \theta_r < 0$. Equations (21) simplify to

$$x_r(t) = x_r(0) + (-v_0^* + v_1^* \cos \theta_r)t \quad (31)$$

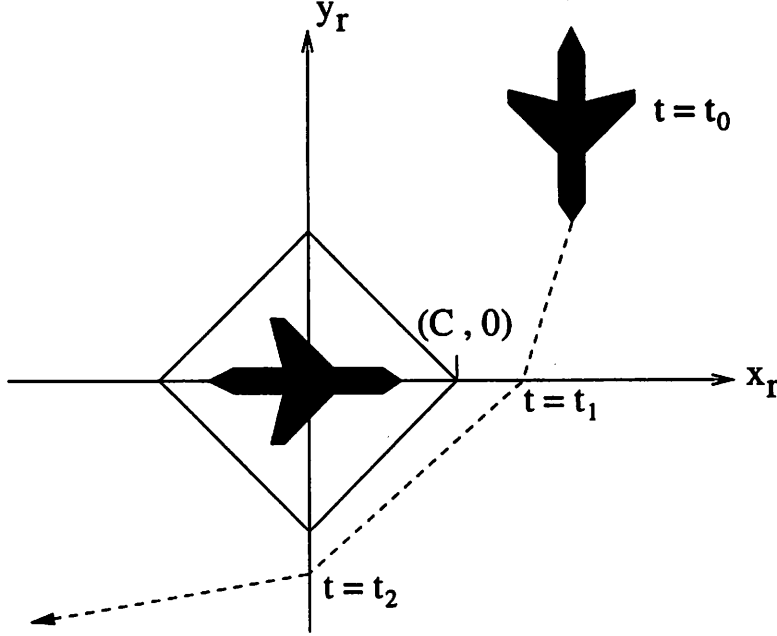


Figure 6: Calculating the safe set of initial conditions for $\theta_r \in (\pi, \frac{3\pi}{2})$

$$y_r(t) = y_r(0) + v_1^* \sin \theta_r t$$

The safe set of initial conditions may be calculated by propagating these equations forward, and determining the restrictions on $(x_r(0), y_r(0))$ so that

$$J(x_r(0), y_r(0), v_0^*, v_1^*) = \inf_{t \geq 0} (|x_r(t)| + |y_r(t)|) \geq C$$

Initially, $x_r(0) > 0$ and $y_r(0) > 0$. By equations (31) and the fact that $v_0^* > 0$, $v_1^* > 0$, $\cos \theta_r < 0$ and $\sin \theta_r < 0$, it is always true that,

$$\begin{aligned} \dot{x}_r(t) &< 0 \\ \dot{y}_r(t) &< 0 \end{aligned} \tag{32}$$

Therefore, the pursuer must either

1. cross the positive x_r axis and then the negative y_r axis, or
2. cross the positive y_r axis and then the negative x_r axis.

From the saddle solution (24,25), it is clear that $v_0^* = \underline{v}_0$ and $v_1^* = \bar{v}_1$. If the pursuer arrives at the x_r axis first, then it will do so at time $t_x = -\frac{y_r(0)}{\bar{v}_1 \sin \theta_r}$, whereas $t_y = -\frac{x_r(0)}{-\underline{v}_0 + \bar{v}_1 \cos \theta_r}$ is the time needed to reach the y_r axis. If $t_x < t_y$ then the pursuer traverses the first route outlined above whereas the second route is traversed if $t_y < t_x$. From now on, it is assumed that the first route is traversed.

Let t_1 represent the time at which the pursuer crosses the positive x_r axis, and t_2 represent the time at which the pursuer crosses the negative y_r axis. Clearly, $t_1 = t_x = -\frac{y_r(0)}{\bar{v}_1 \sin \theta_r}$. In the time interval $0 \leq t \leq t_1$, the saddle solution is

$$\begin{aligned} x_r(t) &= x_r(0) - \underline{v}_0 t \\ y_r(t) &= y_r(0) - \bar{v}_1 t \end{aligned} \tag{33}$$

No collision occurs if

$$\inf_{0 \leq t \leq t_1} (|x_r(0) + (-\underline{v}_0 + \bar{v}_1 \sin \theta_r)t| + |y_r(0) + \bar{v}_1 \sin \theta_r t|) \geq C \quad (34)$$

Since for all time $\dot{x}_r < 0$ and $\dot{y}_r < 0$, the infimum occurs at $t = t_1$. But $y_r(t_1) = 0$ and $x_r(t_1) > 0$ which simplify (34) to

$$x_r(0) + (-\underline{v}_0 + \bar{v}_1 \cos \theta_r)t_1 \geq C \Rightarrow x_r(0) - (-\underline{v}_0 + \bar{v}_1 \cos \theta_r)\frac{y_r(0)}{\bar{v}_1 \sin \theta_r} - C \geq 0 \quad (35)$$

Therefore, collision in the time interval $0 \leq t \leq t_1$ is guaranteed if the initial conditions lie in the half plane

$$S_1 = \{(x_r(0), y_r(0)) \in \mathbb{R}^2 \mid x_r(0) - \frac{-\underline{v}_0 + \bar{v}_1 \cos \theta_r}{\bar{v}_1 \sin \theta_r} y_r(0) - C \geq 0\} \quad (36)$$

At $t = t_1$, depending on the relative strength of $\cos \theta_r$ and $\sin \theta_r$, the control policy either remains the same or switches to

$$\begin{aligned} v_0^* &= \underline{v}_0 \\ v_1^* &= \underline{v}_1 \end{aligned}$$

Assuming that the policy switches, the condition for no collisions in the time interval $t_1 < t \leq t_2$ is

$$\inf_{t_1 \leq t \leq t_2} (|x_r(t_1) + (-\underline{v}_0 + \underline{v}_1 \cos \theta_r)(t - t_1)| + |y_r(t_1) + \underline{v}_1 \cos \theta_r(t - t_1)|) \geq C \quad (37)$$

Due to linearity, the infimum either occurs at $t = t_1$ or at $t = t_2$. Since the system was safe at $t = t_1$ from the above calculations, checking safety at $t = t_2$ is sufficient. At $t = t_2$, $x_r(t_2) = 0$ and $y_r(t_2) < 0$. Thus, (37) reduces to

$$-y_r(t_1) - \underline{v}_1 \sin \theta_r(t_2 - t_1) \geq C \quad (38)$$

But $y_r(t_1) = 0$, $t_2 = t_1 + \frac{x_r(t_1)}{-\underline{v}_0 + \underline{v}_1 \cos \theta_r}$, $x_r(t_1) = x_r(0) + (-\underline{v}_0 + \bar{v}_1 \cos \theta_r)t_1$ and $t_1 = -\frac{y_r(0)}{\bar{v}_1 \sin \theta_r}$. Substituting in (38) results in the following condition on the initial conditions

$$\frac{-\underline{v}_1 \sin \theta_r}{-\underline{v}_0 + \underline{v}_1 \cos \theta_r} x_r(0) + \frac{\underline{v}_1 (-\underline{v}_0 + \bar{v}_1 \cos \theta_r)}{\bar{v}_1 (-\underline{v}_0 + \underline{v}_1 \cos \theta_r)} y_r(0) - C \geq 0 \quad (39)$$

Therefore, collision is avoided in the time interval $t_1 \leq t \leq t_2$ if the initial conditions lie in the half plane

$$S_2 = \{(x_r(0), y_r(0)) \in \mathbb{R}^2 \mid \frac{-\underline{v}_1 \sin \theta_r}{-\underline{v}_0 + \underline{v}_1 \cos \theta_r} x_r(0) + \frac{\underline{v}_1 (-\underline{v}_0 + \bar{v}_1 \cos \theta_r)}{\bar{v}_1 (-\underline{v}_0 + \underline{v}_1 \cos \theta_r)} y_r(0) - C \geq 0\} \quad (40)$$

Using the same line of thought, it is clear that after t_2 , the distance between the two agents is strictly increasing and therefore places no additional constraints on the initial conditions.

The calculations for the safe sets of initial conditions for all three time intervals are summarized in Table 1. The intersection of S_1 and S_2 is the safe set of initial conditions in the first quadrant. A computer program was written to calculate the *unsafe* sets of initial conditions $((x_r(0), y_r(0))$ which result in a collision) for prespecified $\theta_r, \underline{v}_0, \bar{v}_0, \underline{v}_1, \bar{v}_1$. Figure 7 illustrates these unsafe sets for a variety of relative angles θ_r . If the initial condition lies in the unsafe set, then the saddle solution results in a collision. In this case, the agents cannot resolve the possible conflict in a noncooperative manner and thus some form of coordination among the agents is necessary.

Time Interval	Safe Set of Initial Conditions
$0 \leq t \leq t_1$	$x_r(0) - \frac{-\underline{v}_0 + \bar{v}_1 \cos \theta_r}{\bar{v}_1 \sin \theta_r} y_r(0) - C \geq 0$
$t_1 < t \leq t_2$	$\frac{-\underline{v}_1 \sin \theta_r}{-\underline{v}_0 + \bar{v}_1 \cos \theta_r} x_r(0) + \frac{\bar{v}_1 (-\underline{v}_0 + \bar{v}_1 \cos \theta_r)}{\bar{v}_1 (-\underline{v}_0 + \bar{v}_1 \cos \theta_r)} y_r(0) - C \geq 0$
$t > t_2$	$x_r(0) > 0, y_r(0) > 0$

Table 1: Safe set of initial conditions for $x_r(0) > 0$, $y_r(0) > 0$, and $\theta_r \in (\pi, \frac{3\pi}{2})$.

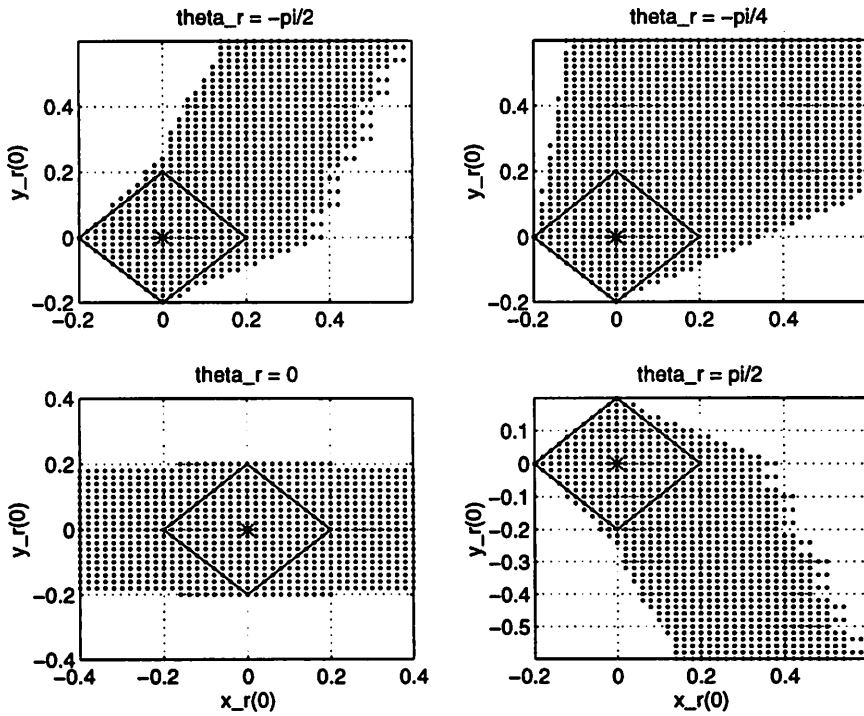


Figure 7: Unsafe sets $(x_r(0), y_r(0))$ for $[\underline{v}_0, \bar{v}_0] = [2, 4]$, $[\underline{v}_1, \bar{v}_1] = [1, 5]$ and $\theta_r = -\pi/2, -\pi/4, 0$, and $\pi/2$. $C = 0.2$.

4.3 Partial Coordination

If the solution to the game of Section 4 is unsafe, meaning that collision occurs for the worst possible disturbance $d^* \in \mathcal{D}$, it may be possible that by reducing the disturbance set to

$$\overline{\mathcal{D}} \subset \mathcal{D}$$

and re-solving the game, the new saddle solution (\bar{u}^*, \bar{d}^*) is safe. The disturbance set may be reduced by *partial coordination* between the agents.

Consider the collision avoidance architecture of Figure 1. If the agents involved in the potential conflict are heterogeneous, then each agent communicates its actions to the agents at a lower priority than its own. In the planar example of (17), this corresponds to $v_1 = v_1^*(t)$ becoming a known function of time. Thus the game becomes the optimal control problem of calculating $v_0 \in \mathcal{U}$ which maximizes the cost function (22). If the initial condition to the optimal control problem is unsafe then full coordination between the agents is necessary.

The more interesting case in a game theoretic sense is the one in which the agents are homogeneous, so that a ranking system does not exist. In this case, each agent calculates the disturbance set $\overline{\mathcal{D}}$ for which a solution to its game exists, and broadcasts this information to all the other agents involved in the collision avoidance procedure. This procedure essentially enlarges the safe set of initial conditions. If the initial condition becomes safe then collision is avoided by restricting the actions of each agent in the smaller disturbance set $\overline{\mathcal{D}}$. If the initial condition is still unsafe then collision is not avoided by partial coordination.

Consider the safe set calculations of the previous section, for the planar example (17). Reduction of \mathcal{D} to $\overline{\mathcal{D}}$ results in larger safe sets of initial conditions. Figure 8 illustrates the unsafe sets corresponding to the situations of Figure 7, with reduced disturbance set $[v_1, \bar{v}_1] = [1.5, 2.5]$. Note that the unsafe sets using the reduced disturbance set are proper subsets of the unsafe sets using the original disturbance sets.

5 Cooperative Conflict Resolution

This section addresses the problem of cooperative conflict resolution among aircraft. This is the kind of collision avoidance scheme which must take place if an aircraft penetrates another aircraft's *alert zone*, which can happen if noncooperative collision avoidance is not sufficient to resolve the conflict between the two aircraft.

An algorithm to predict conflict between pairs of aircraft trajectories is first described. The algorithm is used to determine whether or not a point of conflict exists between the trajectories; if it does, the information is used in the cooperative conflict resolution algorithm.

Cooperative collision avoidance involves a direction change for at least one of the aircraft involved in the conflict. Chosen for its simplicity and inspired by [25], the path deviation for each pairwise conflict is chosen to be two consecutive heading changes resulting in a triangular deviation from the desired path as shown in Figure 10. For a conflict involving three or more aircraft, a scheme which guides each aircraft along a circular path around the conflict point is proposed.

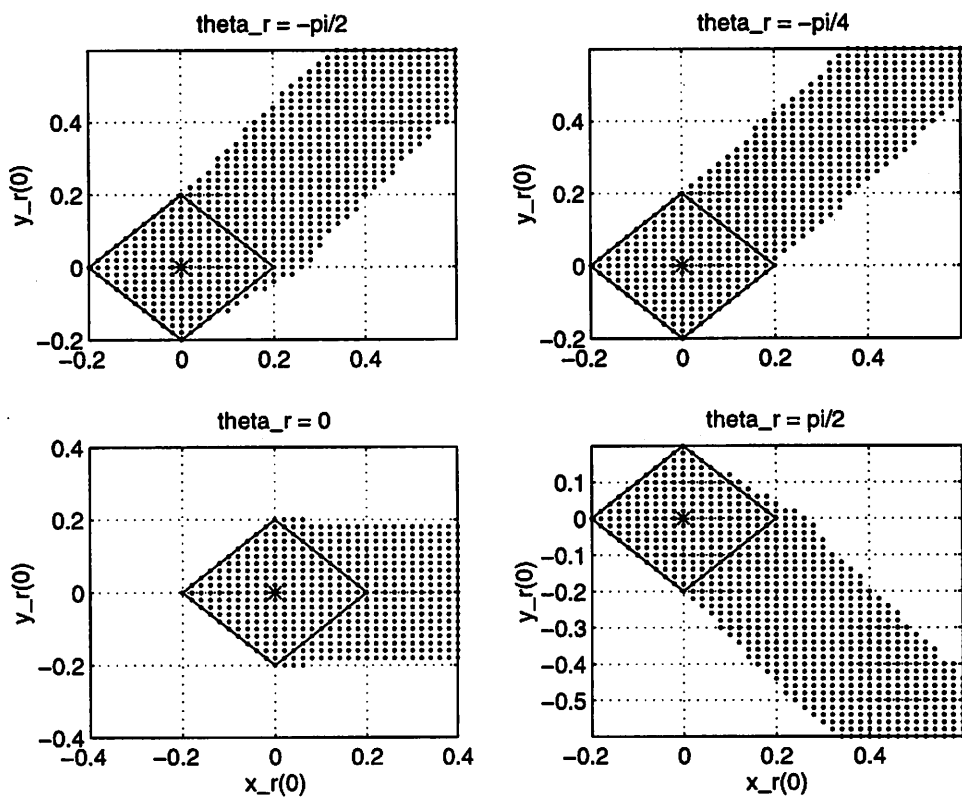


Figure 8: Reduced unsafe sets $(x_r(0), y_r(0))$ for reduced disturbance set $[u_1, \bar{v}_1] = [1.5, 2.5]$

5.1 Conflict Prediction

Conflict prediction is impossible unless one aircraft has some idea of the intentions of another aircraft. In this section, it is assumed that aircraft are cruising in straight lines at a constant altitude, with constant velocity (a valid assumption in the relatively sparse *en route* airspace away from the airport airspace). The velocities and headings of both aircraft involved in the conflict are assumed to be known by each aircraft: once an aircraft enters the alert zone of another aircraft, it transmits its heading and velocity information. This defines its course of action over a certain time horizon which enables the prediction of possible collisions.

With these assumptions, the relative model is

$$\begin{aligned}\dot{x}_r &= -v_0 + v_1 \cos \theta_r \\ \dot{y}_r &= v_1 \sin \theta_r \\ \dot{\theta}_r &= 0\end{aligned}\tag{41}$$

which is model (8) with $\omega_0 = \omega_1 = 0$. Since v_0, v_1 and θ_r are known and assumed to be constant, equations (41) may be solved explicitly. Consider the Euclidean distance between two aircraft given by

$$J_s(t) = \sqrt{x_r^2(t) + y_r^2(t)}\tag{42}$$

and recall that a collision is defined to be the nonempty intersection of the protected zones of two aircraft. If the radius of the protected zone is r , then two protected zones will intersect if and only if the distance between the two aircraft is less than or equal to $2r$, ie. when $J_s(t) \leq 2r$. Therefore, a collision occurs if there exists a time t^* such that $J_s(t^*) \leq 2r$ and a collision is avoided if for all time t , $J_s(t) > 2r$. Clearly if $\min_{t \geq 0} J_s(t) > 2r$ then $J_s(t) \geq 2r$ for all time. The algorithm, therefore, first minimizes $J_s(t)$ over all positive time.

Proposition 3 Given $x_r(t)$ and $y_r(t)$ by

$$\begin{aligned}x_r(t) &= x_r(0) + (-v_0 + v_1 \cos \theta_r)t \\ y_r(t) &= y_r(0) + v_1 \sin \theta_r t\end{aligned}\tag{43}$$

the global minimum value of

$$J_s(t) = \sqrt{x_r^2(t) + y_r^2(t)}$$

over all positive time occurs at

$$t^* = \arg \min_{t \geq 0} J_s(t) = \begin{cases} -\frac{a_1}{2a_2} & \text{if } a_2 \neq 0 \text{ and } \frac{-a_1}{2a_2} \geq 0 \\ 0 & \text{if } a_2 \neq 0 \text{ and } \frac{-a_1}{2a_2} < 0 \\ \Re^+ & \text{if } a_2 = 0 \end{cases}\tag{44}$$

and the minimizing value is given by

$$J_s^* = \min_{t \geq 0} J_s(t) = \begin{cases} \sqrt{-\frac{a_1^2 + 4a_0a_2}{4a_2}} & \text{if } a_2 \neq 0 \text{ and } t^* \geq 0 \\ \sqrt{a_0} = J_s(0) & \text{otherwise} \end{cases}\tag{45}$$

where a_2, a_1 and a_0 are defined as

$$\begin{aligned}a_2 &= v_1^2 \sin^2 \theta_r + (v_1 \cos \theta_r - v_0)^2 \\ a_1 &= 2x_r(0)(v_1 \cos \theta_r - v_0) + 2y_r(0)v_1 \sin \theta_r \\ a_0 &= x_r^2(0) + y_r^2(0) = J_s(0)\end{aligned}\tag{46}$$

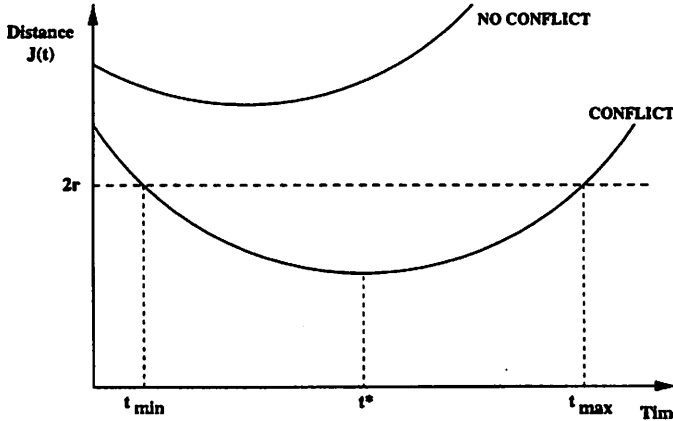


Figure 9: Conflict Prediction

Proof: In Appendix. \square

Proposition 3 enables prediction of whether or not a collision between two aircraft will occur. Once heading and velocity information has been broadcast, the minimum distance J_s^* between two aircraft is analytically computed. If $J_s^* > 2r$, then the protected zones of the two aircraft will not intersect as shown in Figure 9, and therefore no collision will occur. If, however, $J_s^* \leq 2r$ then a conflict is possible. If $J_s^* \leq 2r$ then the time and place of possible collision must be determined. Although the distance between the aircraft reaches its minimum at t^* , $J_s(t)$ is below the safety distance of $2r$ from t_{min} to t_{max} , where t_{min} and t_{max} are the solutions of the equation $J_s(t) = 2r$ which can be converted to the simple quadratic equation $J_s^2(t) = 4r^2$. The protected zones first touch each other at time t_{min} and then overlap until time t_{max} after which they have empty intersection. Times t_{min} and t_{max} can be easily computed by the formula

$$t_{min,max} = \frac{-a_1 \pm \sqrt{a_1^2 - 4a_2(a_2 - 4r^2)}}{2a_2} \quad (47)$$

If $J_s^* \leq 2r$, it is geometrically clear from Figure 9 that two real solutions exist. Equivalently, it can be shown that the discriminant of the quadratic is always positive. Furthermore, if $a_0 = J_s(0) \geq 2r$ then it can be shown that $t_{max} \geq t_{min} \geq 0$. In the degenerate case when $a_2 = 0$ then $J_s(t) = J_s(0)$ and thus either $J_s(t) = J_s(0) < 2r$ in which case the two aircraft have already collided or $J_s(t) = J_s(0) \geq 2r$ in which case the two aircraft will never collide.

Once the projected time of conflict has been determined, the position of the possible collision can be obtained by simply integrating the model of an aircraft in absolute coordinates (1),(2).

5.2 Protocol for Two Aircraft

A general short range conflict scenario is depicted in Figure 10. Aircraft 1 with speed v_1 and initial heading θ_r has desired relative trajectory $(x_r^d(t), y_r^d(t))$, which is the straight line path joining point A and point C a distance d away from the origin (seen as the dotted line in Figure 10). To simplify the analysis, the protected zone of aircraft 1 is translated to aircraft 0, to make the protected zone around aircraft 0 twice its original radius. If aircraft 1 were to continue along its original desired path, it would cut through this protected zone, and come into conflict with aircraft 0. To avoid

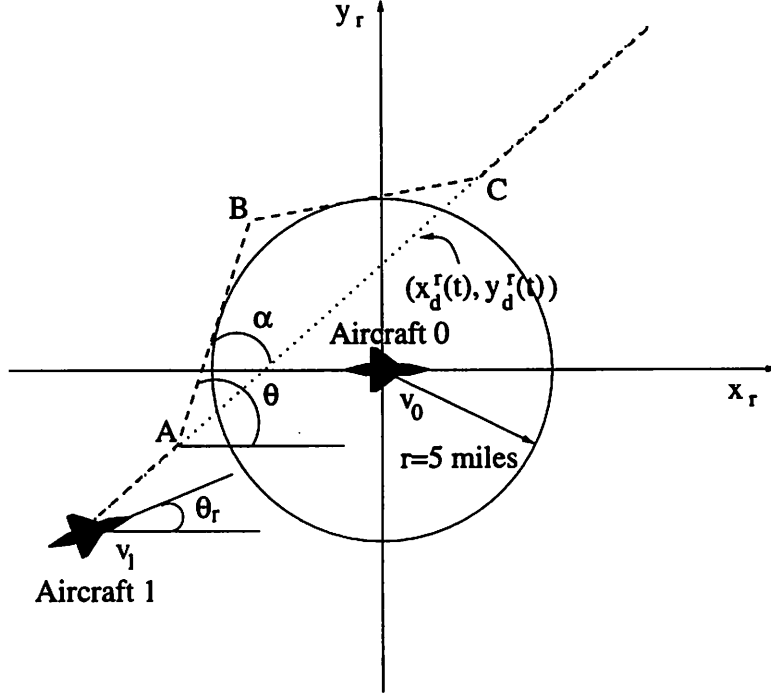


Figure 10: Showing the triangular path deviation (dashed line), at optimal angle θ^* , to be used in pairwise conflict avoidance

the protected zone, the proposed deviation for aircraft 1 is the triangular path ABC tangent to the protected zone at two places and parameterized by the deviation angle θ (represented by the dashed line in Figure 10).

Aircraft 1 follows the specified path ABC if the component of its relative velocity normal to this path is zero. Since straight line paths are considered, the relative velocity of aircraft 1 is described by the model (17). The angle θ is calculated to minimize the time it takes for aircraft 1 to travel along the path ABC . Its optimal value is obtained by minimizing with respect to θ the length of ABC divided by the speed of the aircraft along this path. Only the path AB need be considered, since by symmetry the path length BC is equal to that of AB .

The component of the relative velocity of aircraft 1 along the path AB may be calculated as:

$$v_{AB} = v_1 \cos(\theta - \theta_r) - v_0 \cos \theta$$

and the component perpendicular to this path, as

$$v_{AB}^\perp = v_1 \sin(\theta - \theta_r) - v_0 \sin \theta$$

The optimal value deviation angle θ^* is therefore

$$\theta^* = \arg \min_{\theta} \frac{|AB|}{v_{AB}} \Big|_{v_{AB}^\perp = 0} \quad (48)$$

where

$$|AB| = \frac{r}{\tan \alpha} - \frac{d}{\sin \alpha} + r \tan \alpha \quad (49)$$

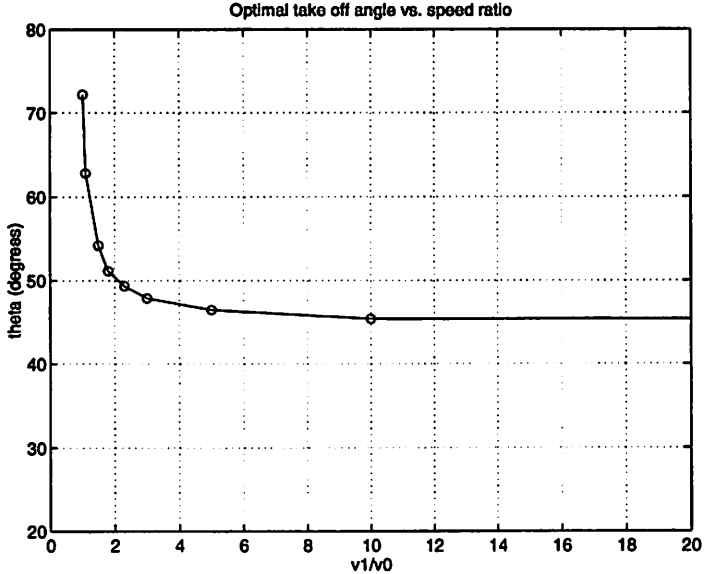


Figure 11: Optimal deviation angle θ^* vs. speed ratio v_1/v_0

and

$$\alpha = \theta - \tan^{-1}(\dot{y}_r/\dot{x}_r) \quad (50)$$

For example, consider the scenario in which aircraft 1 has the same initial heading as aircraft 0 ($\theta_r = 0$), and its original desired path is along the x_r axis ($d = 0$). A potential conflict exists if v_1 is greater than v_0 . The minimum time triangular maneuver to avoid conflict, called an *Overtake maneuver* in this case, may be calculated using (48):

Proposition 4 (Overtake Maneuver) *For an Overtake, in which aircraft 1 is approaching aircraft 0 from behind with a greater speed, the minimum time triangular maneuver for aircraft 1 approaches a departure angle of $\theta \rightarrow 45^\circ$ from the horizontal, as the speed ratio $v_1/v_0 \rightarrow \infty$.*

Proof: In Appendix. \square

This makes sense intuitively: a deviation angle of 45° means that aircraft 1 remains on the horizontal path with $\theta_r = 0$ for as long as possible, since the speed differential between v_1 and v_0 is greatest along this path. Figure 11 shows a plot of the θ^* for various speed ratios v_1/v_0 . Figure 12 illustrates the distance from the origin at which the deviation maneuver should begin. For a protected zone radius of 5 miles, this distance approaches $5\sqrt{2}$, or 7.07, miles.

The *Overtake maneuver* is a special case of the general class of triangular conflict resolution maneuvers described by equations (48), (49), and (50). In each aircraft's FVMS, a routine exists which computes θ^* for the different parameters r , d , θ_r , and v_1/v_0 :

$$\theta^* = \text{Overtake}(r, d, \theta_r, v_1/v_0) \quad (51)$$

It is assumed in this architecture that the aircraft with the greater speed must perform the maneuver; the other aircraft remains on its original course.

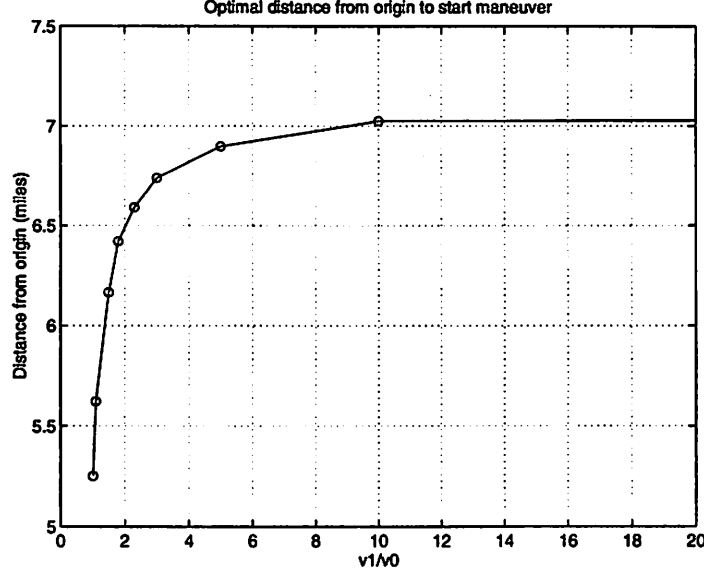


Figure 12: Optimal distance from origin to start maneuver vs. speed ratio v_1/v_0

Consider now a *HeadOn* conflict, in which aircraft 1 is heading towards aircraft 0 ($\theta_r = 180^\circ$) along the x_r axis ($d = 0$). A potential conflict exists regardless of the speeds of aircraft 0 and aircraft 1. Although the conflict may be resolved using the general maneuver discussed above, the issue of *fairness* arises. If $v_1 \approx v_0$, it is not clear how to choose which aircraft deviates from its original trajectory. A natural solution is to define a maneuver in which both aircraft deviate from their original trajectories:

$$(\theta_0^*, \theta_1^*) = \text{HeadOn}(r, d, \theta_r, v_1/v_0) \quad (52)$$

Inspired by the Overtake maneuver, θ_0^* and θ_1^* are set to 45° and -45° , respectively, when $d = 0$ and $\theta_r = 180^\circ$. The Overtake maneuver is *safe by design*, since the construction of the deviation path explicitly avoids the protected zone of one of the aircraft. In order to ensure that the HeadOn conflict is safe by design, both aircraft must deviate a horizontal distance of 5 miles (the minimum aircraft separation) away from their original paths. Figure 13 illustrates why, in the absolute frame of the two aircraft. Aircraft 1 must be 5 miles away from aircraft 0 for all v_1/v_0 . In particular, if v_0 were much greater than v_1 , and aircraft 0 ended up at point C in Figure 13 before aircraft 1 had left point D , then points C and D must be 5 miles apart. This is clearly not optimal, since it is worse than the previous case in which only one of the aircraft has to deviate a horizontal distance of $5\sqrt{2}$ miles. It is difficult to prove that less conservative designs, in which the horizontal deviation for each aircraft is less than 5 miles, are *a priori* safe for various speed ratios, unless a formal verification tool such as Cospan [26] or HyTech [4] is used. This type of tool automates a mathematical proof that, for given sets of initial conditions and constraints on the system variables, certain states will or will not be reached. For the maneuver discussed here, such a tool could be used to verify that the positions of the aircraft do not come within 5 miles of each other. The particular tool which has been used to verify similar maneuvers is the Hybrid system verification tool HyTech [27].

As with the Overtake maneuver, the HeadOn maneuver in its general form may be used for relative headings θ_r other than 180° . Figure 14 illustrates the partitioning of all two-aircraft, same-altitude conflicts as either Overtake or HeadOn, depending on the relative position and angle of the two

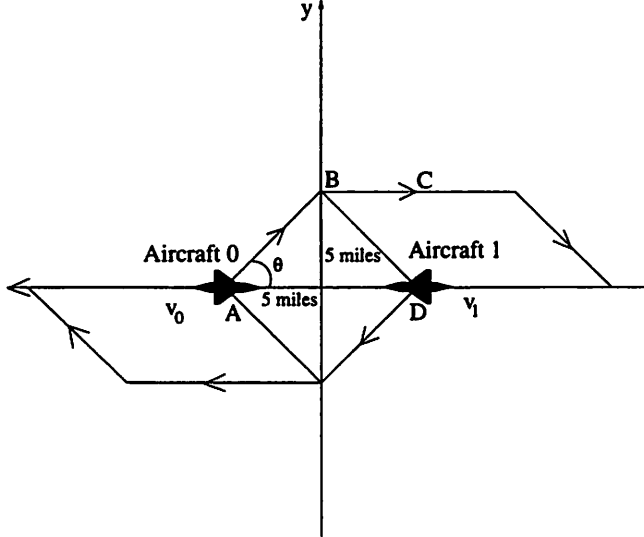


Figure 13: Showing the HeadOn conflict and subsequent conflict resolution maneuver

aircraft.

Once the Overtake or HeadOn maneuver is complete, a *Catch Up* maneuver is performed by the aircraft, to catch up to their original trajectories in time.

5.3 Protocol for Three Aircraft

For three aircraft coming into potential conflict, there are many more possibilities for types of conflict. For example, two aircraft could have intersecting trajectories, and then conflict resolution between these two could result in a new conflict with a third aircraft. Pairwise conflict resolution may not work in cases such as these: it is worthwhile to design a maneuver which works for three aircraft, with the possibility to extend it to more than three aircraft. A maneuver which is inspired by the traffic rotaries on the ground is the *Roundabout* maneuver, illustrated in Figure 15 for the case of three aircraft with two initial points of conflict. For this maneuver, a circular path is defined around the conflict points of all three trajectories as shown. The aircraft are restricted to fly along the circular path segments with a given speed, as not to overtake the other aircraft already involved in the maneuver. An aircraft may not enter the Roundabout until the other aircraft are outside its protected zone; in extreme cases this may force an aircraft to enter a holding pattern to delay its entry.

Figure 16 depicts the hybrid automaton describing the conflict resolution architecture described in this paper. If noncooperative conflict resolution (described by the hybrid automaton of Figure 4) results in an unsafe solution, then cooperative collision resolution involving one of the three maneuvers described in this section must be invoked. Once the maneuvers are complete, the aircraft enter the *Catch Up* mode, and the system returns to its original *No conflict* state. Once again, HyTech is used to verify the safety of the protocols.

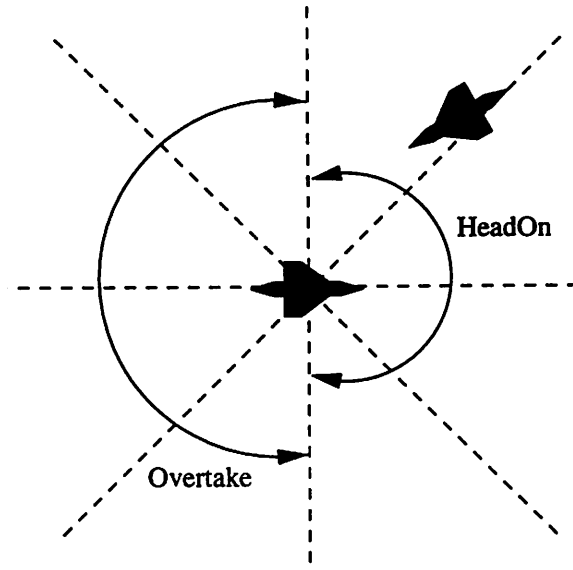


Figure 14: Conflicts: *Overtake* and *HeadOn*

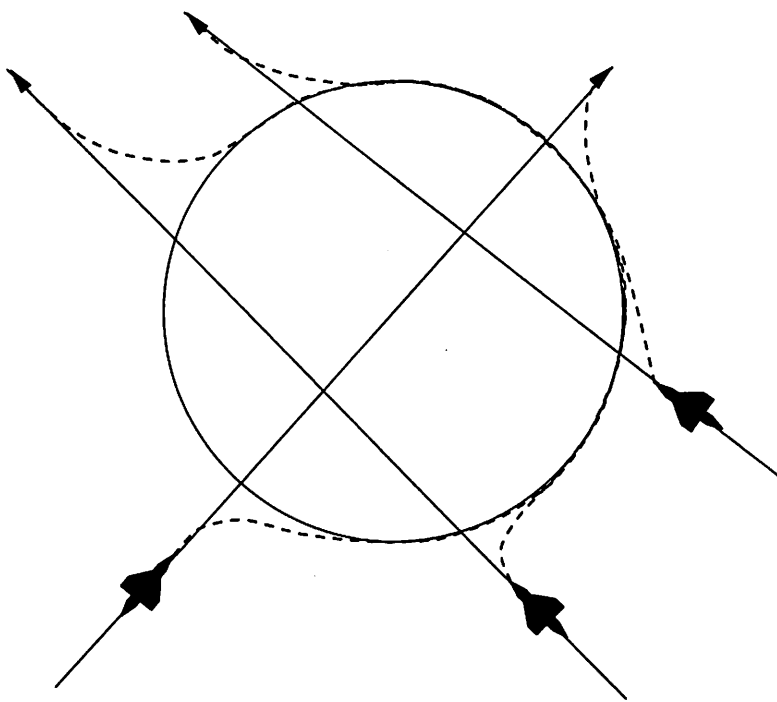


Figure 15: Conflict Resolution for three aircraft: the Roundabout maneuver

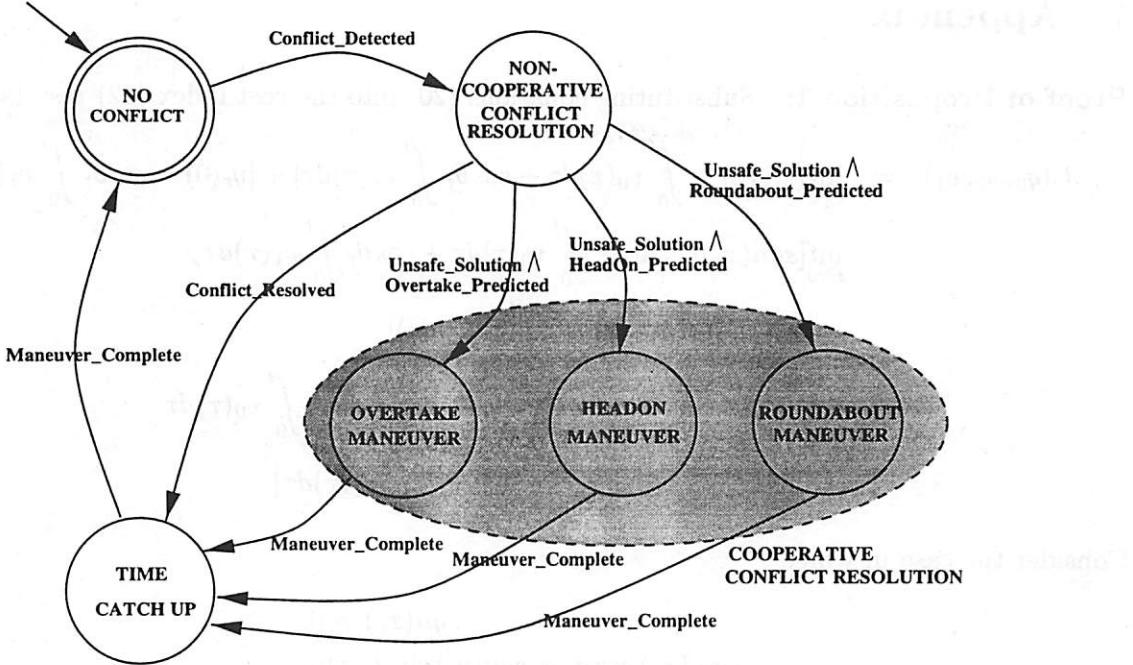


Figure 16: Hybrid Automaton describing Conflict Resolution

6 Conclusions

In this paper, a conflict resolution architecture for multi-agent systems has been presented. The architecture consists of both a noncooperative collision avoidance scheme based on game theory, as well as a cooperative scheme based on inter-agent coordination. The architecture was illustrated using a two-agent, planar example which arises frequently in air traffic systems. For long range collision avoidance, a saddle solution to the noncooperative game was found and the safe set of initial conditions was computed. For short range collision avoidance, protocols involving Overtake and HeadOn conflict resolution involving coordination between multiple aircraft were derived. Extensions to multiple aircraft coordination were also suggested. They can be verified using, for example HyTech. The protocols involving coordination were suggestive of Nash equilibria for non-competitive games. In future work, this will be worked out in detail, along with information exchange requirements.

Current research topics include the extension of our planar example (without turning) to the planar example with turning included as well as collision resolution in three dimensional space. Non competitive games with n-players will be considered as well, with the design doing its best to minimize the level of verification required in subsequent stages, using conventional tools such as HyTech or Cospan.

7 Appendix

Proof of Proposition 1: Substituting equations (20) into the cost index (22) results in

$$\begin{aligned}
J_s(q_0, v_0, v_1) &= \inf_{t \geq 0} \left(|x_r(0) - \int_0^t v_0(\tau) d\tau + \cos \theta_r \int_0^t v_1(\tau) d\tau| + |y_r(0) + \sin \theta_r \int_0^t v_1(\tau) d\tau| \right) \\
&= \inf_{t \geq 0} \left[sgn(x_r)(x_r(0) - \int_0^t v_0(\tau) d\tau + \cos \theta_r \int_0^t v_1(\tau) d\tau) \right. \\
&\quad \left. + sgn(y_r)(y_r(0) + \sin \theta_r \int_0^t v_1(\tau) d\tau) \right] \\
&= \inf_{t \geq 0} \left[sgn(x_r)x_r(0) + sgn(y_r)y_r(0) - sgn(x_r) \int_0^t v_0(\tau) d\tau \right. \\
&\quad \left. + (sgn(x_r)\cos \theta_r + sgn(y_r)\sin \theta_r) \int_0^t v_1(\tau) d\tau \right]
\end{aligned}$$

Consider the case in which

$$\begin{aligned}
sgn(x_r) &> 0 \\
sgn(x_r)\cos \theta_r + sgn(y_r)\sin \theta_r &> 0
\end{aligned}$$

We will show that in this case the saddle solution is $v_0^* = \underline{v}_0$ and $v_1^* = \underline{v}_1$. Then,

$$\begin{aligned}
J_s(q_0, v_0^*, v_1^*) &= \inf_{t \geq 0} \left[sgn(x_r)x_r(0) + sgn(y_r)y_r(0) - sgn(x_r)\underline{v}_0 t \right. \\
&\quad \left. + (sgn(x_r)\cos \theta_r + sgn(y_r)\sin \theta_r)\underline{v}_1 t \right]
\end{aligned}$$

Now let $v_1 = v_1^*$ and vary v_0 . Then

$$\begin{aligned}
J_s(q_0, v_0, v_1^*) &= \inf_{t \geq 0} \left[sgn(x_r)x_r(0) + sgn(y_r)y_r(0) - sgn(x_r) \int_0^t v_0(\tau) d\tau \right. \\
&\quad \left. + (sgn(x_r)\cos \theta_r + sgn(y_r)\sin \theta_r)\underline{v}_1 t \right]
\end{aligned}$$

But we have $v_0 = \underline{v}_0 + \delta v_0$ where $\delta v_0 \geq 0$. Therefore

$$\begin{aligned}
J_s(q_0, v_0, v_1^*) &= \inf_{t \geq 0} \left[sgn(x_r)x_r(0) + sgn(y_r)y_r(0) - sgn(x_r)\underline{v}_0 t - sgn(x_r) \int_0^t \delta v_0(\tau) d\tau \right. \\
&\quad \left. + (sgn(x_r)\cos \theta_r + sgn(y_r)\sin \theta_r)\underline{v}_1 t \right] \\
&\leq \inf_{t \geq 0} \left[sgn(x_r)x_r(0) + sgn(y_r)y_r(0) - sgn(x_r)\underline{v}_0 t \right. \\
&\quad \left. + (sgn(x_r)\cos \theta_r + sgn(y_r)\sin \theta_r)\underline{v}_1 t \right] \\
&= J_s(q_0, v_0^*, v_1^*)
\end{aligned}$$

since both $sgn(x_r) > 0$ and $\delta v_0 \geq 0$. Similarly, let $v_0 = v_0^*$ and vary v_1 . Then $v_1 = \underline{v}_1 + \delta v_1$ with $\delta v_1 \geq 0$. Thus

$$\begin{aligned}
J_s(q_0, v_0^*, v_1) &= \inf_{t \geq 0} \left[sgn(x_r)x_r(0) + sgn(y_r)y_r(0) - sgn(x_r)\underline{v}_0 t \right. \\
&\quad \left. + (sgn(x_r)\cos \theta_r + sgn(y_r)\sin \theta_r) \int_0^t v_1(\tau) d\tau \right] \\
&= \inf_{t \geq 0} \left[sgn(x_r)x_r(0) + sgn(y_r)y_r(0) - sgn(x_r)\underline{v}_0 t \right]
\end{aligned}$$

$$\begin{aligned}
& + (sgn(x_r) \cos \theta_r + sgn(y_r) \sin \theta_r) \underline{v}_1 t + (sgn(x_r) \cos \theta_r + sgn(y_r) \sin \theta_r) \int_0^t \delta v_1(\tau) d\tau] \\
\geq & \inf_{t \geq 0} [sgn(x_r) x_r(0) + sgn(y_r) y_r(0) - sgn(x_r) \underline{v}_0 t + (sgn(x_r) \cos \theta_r + sgn(y_r) \sin \theta_r) \underline{v}_1 t] \\
& + \inf_{t \geq 0} [(sgn(x_r) \cos \theta_r + sgn(y_r) \sin \theta_r) \int_0^t \delta v_1(\tau) d\tau] \\
\geq & J_s(q_0, v_0^*, v_1^*)
\end{aligned}$$

since $(sgn(x_r) \cos \theta_r + sgn(y_r) \sin \theta_r) > 0$ and, in general, $\inf_{t \geq 0} (x_1 + x_2) \geq \inf_{t \geq 0} x_1 + \inf_{t \geq 0} x_2$. Summarizing, we have shown above that in this case,

$$J_s(q_0, v_0, v_1^*) \leq J_s(q_0, v_0^*, v_1^*) \leq J_s(q_0, v_0^*, v_1) \quad (53)$$

Therefore, $v_0^* = \underline{v}_0$, $v_1^* = \underline{v}_1$ is a saddle solution in this case. The three other cases can be shown in a similar manner. \square

Proof of Proposition 2: Consider first the x_r -axis. The switching function in this case is simply $S(x_r, y_r, \theta_r) = y_r$. The evolution of S in the regions $y_r > 0$ and $y_r < 0$ is given by

$$\begin{aligned}
\frac{dS}{dt} \Big|_+ &= \dot{y}_r = v_1^+ \sin \theta_r \\
\frac{dS}{dt} \Big|_- &= \dot{y}_r = v_1^- \sin \theta_r
\end{aligned}$$

where v_1^+ is the control law in region $y_r > 0$ and v_1^- is the control law in region $y_r < 0$. From equation (25) it is clear that v_1^+ and v_1^- are either \underline{v}_1 or \bar{v}_1 depending on the relative orientation θ_r . If θ_r is such that $sgn(\sin(\theta_r + \frac{\pi}{4})) = sgn(\sin(\theta_r - \frac{\pi}{4}))$ then from equation (25,26) we obtain that $(v_1^+, v_1^-) = (\bar{v}_1, \bar{v}_1)$ or $(v_1^+, v_1^-) = (\underline{v}_1, \underline{v}_1)$ in which case there is no switching at all since $\frac{dS}{dt} \Big|_+$ and $\frac{dS}{dt} \Big|_-$ have the same sign. In this case the pursuer simply crosses through the surface of discontinuity and no chattering is possible.

If, however, θ_r is such that $sgn(\sin(\theta_r + \frac{\pi}{4})) \neq sgn(\sin(\theta_r - \frac{\pi}{4}))$ then $(v_1^+, v_1^-) = (\bar{v}_1, \underline{v}_1)$ or $(v_1^+, v_1^-) = (\underline{v}_1, \bar{v}_1)$. Thus, the pursuer switches policy once the x_r -axis is crossed. Consider first the case where $(v_1^+, v_1^-) = (\underline{v}_1, \bar{v}_1)$. Then

$$\begin{aligned}
\frac{dS}{dt} \Big|_+ &= \dot{y}_r = \underline{v}_1 \sin \theta_r \\
\frac{dS}{dt} \Big|_- &= \dot{y}_r = \bar{v}_1 \sin \theta_r
\end{aligned}$$

Chattering will occur when $\frac{dS}{dt} \Big|_+ < 0$ and $\frac{dS}{dt} \Big|_- > 0$ or equivalently when $\underline{v}_1 \sin \theta_r < 0$ and $\bar{v}_1 \sin \theta_r > 0$. Clearly, if $\sin \theta_r = 0$ then chattering is not possible. If $\sin \theta_r > 0$ then chattering is possible only if $\underline{v}_1 < 0$ and $\bar{v}_1 > 0$ whereas if $\sin \theta_r < 0$ then chattering is possible under the infeasible conditions $\underline{v}_1 > 0$ and $\bar{v}_1 < 0$. Therefore, if $(v_1^+, v_1^-) = (\underline{v}_1, \bar{v}_1)$, then chattering is possible only when $\sin \theta_r > 0$ and $\underline{v}_1 < 0 < \bar{v}_1$.

Considering in a similar manner the second case where $(v_1^+, v_1^-) = (\bar{v}_1, \underline{v}_1)$, we obtain that chattering is possible only when $\sin \theta_r < 0$ and $\underline{v}_1 < 0 < \bar{v}_1$. Grouping the two conditions together we obtain that the x_r -axis is a chattering surface only if $\sin \theta_r \neq 0$ and $\underline{v}_1 < 0 < \bar{v}_1$.

In the case of the y_r -axis, the switching function is $S(x_r, y_r, \theta_r) = x_r$. The evolution of S in the regions $x_r > 0$ and $x_r < 0$ is given by

$$\begin{aligned}\frac{dS}{dt} \Big|_+ &= \dot{x}_r = -v_0^+ + v_1^+ \cos \theta_r \\ \frac{dS}{dt} \Big|_- &= \dot{x}_r = -v_0^- + v_1^- \cos \theta_r\end{aligned}$$

From the control law (24) it is clear that $v_0^+ = \underline{v}_0$ and $v_0^- = \bar{v}_0$ since the evader always changes policy in the two regions. Again, the pursuer will change policy depending on whether the relative orientation θ_r satisfies the condition $\operatorname{sgn}(\sin(\theta_r + \frac{\pi}{4})) = \operatorname{sgn}(\sin(\theta_r - \frac{\pi}{4}))$ or not.

If θ_r is such that from equation (25) the pursuer's policy remains the same, then either $(v_1^+, v_1^-) = (\bar{v}_1, \bar{v}_1)$ or $(v_1^+, v_1^-) = (\underline{v}_1, \underline{v}_1)$. In both of these cases, a simple calculation shows that it is impossible to have $\frac{dS}{dt} \Big|_+ < 0$ and $\frac{dS}{dt} \Big|_- > 0$ since either

$$\begin{aligned}\frac{dS}{dt} \Big|_+ < 0 &\Rightarrow -\underline{v}_0 + \underline{v}_1 \cos \theta_r < 0 \\ \frac{dS}{dt} \Big|_- > 0 &\Rightarrow -\bar{v}_0 + \underline{v}_1 \cos \theta_r > 0\end{aligned}$$

in which case the infeasible condition $\bar{v}_0 < \underline{v}_1 \cos \theta_r < \underline{v}_0$ must be satisfied or

$$\begin{aligned}\frac{dS}{dt} \Big|_+ < 0 &\Rightarrow -\underline{v}_0 + \bar{v}_1 \cos \theta_r < 0 \\ \frac{dS}{dt} \Big|_- > 0 &\Rightarrow -\bar{v}_0 + \bar{v}_1 \cos \theta_r > 0\end{aligned}$$

in which case $\bar{v}_0 < \bar{v}_1 \cos \theta_r < \underline{v}_0$ must be satisfied. Therefore, in both cases chattering solutions are not possible.

If, however, θ_r is such that $\operatorname{sgn}(\sin(\theta_r + \frac{\pi}{4})) \neq \operatorname{sgn}(\sin(\theta_r - \frac{\pi}{4}))$ then by (25,26) the pursuer changes policy by crossing the y_r -axis. Then either $(v_1^+, v_1^-) = (\bar{v}_1, \underline{v}_1)$ or $(v_1^+, v_1^-) = (\underline{v}_1, \bar{v}_1)$. In the first case, the pursuer switches policy from $v_1 = \underline{v}_1$ in the region $x_r < 0$ to $v_1 = \bar{v}_1$ in $x_r > 0$. In this case, we can have $\frac{dS}{dt} \Big|_+ < 0$ and $\frac{dS}{dt} \Big|_- > 0$ only if

$$\begin{aligned}\frac{dS}{dt} \Big|_+ < 0 &\Rightarrow -\underline{v}_0 + \bar{v}_1 \cos \theta_r < 0 \\ \frac{dS}{dt} \Big|_- > 0 &\Rightarrow -\bar{v}_0 + \underline{v}_1 \cos \theta_r > 0\end{aligned}$$

which after simple calculations can be shown to be feasible only if

$$\begin{aligned}\cos \theta_r &< 0 \\ \underline{v}_1 \cos \theta_r &> \bar{v}_0 \\ \bar{v}_1 \cos \theta_r &< \underline{v}_0\end{aligned}$$

Similarly, for the case where $(v_1^+, v_1^-) = (\underline{v}_1, \bar{v}_1)$, chattering is possible if

$$\begin{aligned}\frac{dS}{dt} \Big|_+ < 0 &\Rightarrow -\underline{v}_0 + \underline{v}_1 \cos \theta_r < 0 \\ \frac{dS}{dt} \Big|_- > 0 &\Rightarrow -\bar{v}_0 + \bar{v}_1 \cos \theta_r > 0\end{aligned}$$

which is feasible only if

$$\begin{aligned}\cos \theta_r &> 0 \\ \bar{v}_1 \cos \theta_r &> \bar{v}_0 \\ v_1 \cos \theta_r &< v_0\end{aligned}$$

If the above conditions do not hold, then the system will simply cross through the the surface of discontinuity. \square

Proof of Proposition 3: Minimizing $J_s(t)$ is equivalent to minimizing $J_s^2(t)$. Inserting equations (43) in the expression for $J_s^2(t)$ results in $J_s^2(t) = a_2 t^2 + a_1 t + a_0$ where a_0 , a_1 and a_2 are defined in (46). The optimal values for t and $J_s(t)$ follow from the Kuhn-Tucker conditions [28]. Note that $a_2 \geq 0$ which results in $J_s^2(t)$ being convex as well as satisfying the sufficient conditions for minimization. Furthermore, the constraint set $t \geq 0$ is also convex. This results in globally minimizing solutions. If $a_2 = 0$ then $a_1 = 0$ and thus $J_s(t) = J_s(0)$ for all time t . This corresponds to the case where $\theta_r = 0$ and $v_2 = v_1$. \square

Proof of Proposition 4: Substituting $\theta_r = 0$ and $d = 0$ into equations (48), (49), and (50), the optimal angle θ^* may be calculated as

$$\theta^* = \arg \min_{\theta} \frac{r}{\sin \theta \cos \theta (v_1 \cos(\theta - \theta_r) - v_0 \cos \theta)} \Big|_{v_1 \sin(\theta - \theta_r) - v_0 \sin \theta = 0} \quad (54)$$

$$= \arg \min_{\theta} \frac{r}{\sin \theta \cos \theta (\sqrt{v_1^2 - v_0^2 \sin^2 \theta} - v_0 \cos \theta)} \quad (55)$$

θ^* is thus calculated as the solutions to the following:

$$(\cos^2 \theta^* - \sin^2 \theta^*) \left(\sqrt{\frac{v_1^2}{v_0^2} - \sin^2 \theta^*} - \cos \theta^* \right) + \sin \theta^* \cos \theta^* \left(-\frac{\sin \theta^* \cos \theta^*}{\sqrt{\frac{v_1^2}{v_0^2} - \sin^2 \theta^*}} + \sin \theta^* \right) = 0 \quad (56)$$

For $v_1 \leq v_0$, (54) has no solution. When $v_1 > v_0$, the solution θ^* depends on the ratio v_1/v_0 , as illustrated in Figure 11. If $v_1/v_0 \gg 1$, then equation (56) may be approximated by

$$(\cos^2 \theta^* - \sin^2 \theta^*) = 0 \quad (57)$$

which has as solution $\theta^* = \pm 45^\circ$ (corresponding to deviating to the left or right of the circle). \square

References

- [1] S. Sastry, G. Meyer, C. Tomlin, J. Lygeros, D. Godbole, and G. Pappas. Hybrid control in air traffic management systems. In *Proceedings of the 1995 IEEE Conference in Decision and Control*, pages 1478–1483, New Orleans, LA, December 1995.
- [2] Pravin Varaiya. Smart cars on smart roads: problems of control. *IEEE Transactions on Automatic Control*, AC-38(2):195–207, 1993.

- [3] R.P. Kurshan. *Computer Aided Verification of Coordinating processes; the automata theoretic approach*. Princeton University Press, 1994.
- [4] Thomas A. Henzinger, Pei-Hsin Ho, and Howard Wong-Toi. *A User Guide to HyTech*. Department of Computer Science, Cornell University, 1996.
- [5] Robert L. Grossman, Anil Nerode, Anders P. Ravn, and Hans Rischel, editors. *Hybrid Systems*. Springer-Verlag, 1993.
- [6] Panos Antsaklis, Wolf Kohn, Anil Nerode, and Shankar Sastry, editors. *Hybrid Systems II*. Springer-Verlag, 1995.
- [7] R. Alur, C. Courcoubetis, and D. Dill. Model checking for real-time systems. *Logic in Computer Science*, pages 414–425, 1990.
- [8] Anuj Puri and Pravin Varaiya. Decidability of hybrid systems with rectangular differential inclusions. In *Computer Aided Verification*, pages 95–104, 1994.
- [9] R.W. Brockett. Hybrid models for motion control systems. In H. Trentelman and J.C. Willems, editors, *Perspectives in Control*, pages 29–54. Birkhauser, Boston, 1993.
- [10] M. Branicky, V. Borkar, and S. Mitter. A unified framework for hybrid control:background, model and theory. Technical Report LIDS-P-2239, Massachusetts Institute of Technology, 1994.
- [11] Akash Deshpande. *Control of Hybrid Systems*. PhD thesis, Department of Electrical Engineering, University of California, Berkeley, California, 1994.
- [12] A. Nerode and W. Kohn. Multiple agent hybrid control architecture. In Robert L. Grossman, Anil Nerode, Anders P. Ravn, and Hans Rischel, editors, *Hybrid Systems*, pages 297–316. Springer Verlag, New York, 1993.
- [13] W. Kohn, A. Nerode, and J. Remmel. Hybrid systems as Finsler manifolds: Finite state control as approximation to connections. In Panos Antsaklis, Wolf Kohn, Anil Nerode, and Shankar Sastry, editors, *Hybrid Systems II*, pages 294–321. Springer Verlag, New York, 1995.
- [14] T. Basar and G. J. Olsder. *Dynamic Non-cooperative Game Theory*. Academic Press, second edition, 1995.
- [15] Joseph Lewin. *Differential Games*. Springer Verlag, 1994.
- [16] John Lygeros, Datta Godbole, and Shankar Sastry. A game theoretic approach to hybrid system design. Technical Report UCB/ERL M95/77, University of California, Berkeley, 1995.
- [17] G. Owen. *Game Theory*. Academic Press, third edition, 1995.
- [18] John Lygeros, Datta N. Godbole, and Shankar Sastry. A design framework for hierarchical, hybrid control. Submitted to IEEE Transactions on Automatic Control, Special Issue on Hybrid Systems, 1996.
- [19] John Lygeros, Datta N. Godbole, and Shankar Sastry. A verified hybrid controller for automated vehicles. Submitted to IEEE Transactions on Automatic Control, Special Issue on Hybrid Systems, 1996.

- [20] Lance Sherry, David Youssefi, and Charles Hynes. A formalism for the specification of operationally embedded reactive avionic systems. Honeywell Publication C695370001, 1995.
- [21] Nicolas Pujet and Eric Feron. Flight plan optimization in flexible air traffic environments. Department of Aeronautics and Astronautics, Massachusetts Institute of Technology, 1995.
- [22] Héctor Sussmann. Shortest 3-dimensional paths with a prescribed curvature bound. In *Proceedings of the 1995 IEEE Conference in Decision and Control*, pages 3306–3312, New Orleans, LA, December 1995.
- [23] L. E. Dubins. On curves of minimal length with a constraint on average curvature, and with prescribed initial and terminal positions and tangents. *American Journal of Mathematics*, 79:497–516, 1957.
- [24] Steven LaValle. *A Game-Theoretic Framework for Robot Motion Planning*. PhD thesis, Department of Electrical Engineering, University of Illinois at Urbana-Champaign, 1995.
- [25] Russell A. Paielli and Heinz Erzberger. Conflict probability estimation and resolution for free flight. NASA Ames Research Center, Preprint, 1996.
- [26] Z. Har’El and R.P. Kurshan. *Cospan User’s Guide*. AT&T Bell Laboratories, 1987.
- [27] Claire Tomlin. Verification of an air traffic management protocol using HyTech. University of California at Berkeley, 1996.
- [28] D. Luenberger. *Linear and Nonlinear Programming*. Addison-Wesley, second edition, 1984.